The EMBO Journal Vol.17 No.2 pp.482–497, 1998

Regulation of the G_1 phase of the cell cycle by periodic stabilization and degradation of the $p25^{rum1}$ CDK inhibitor

Javier Benito, Cristina Martín-Castellanos and Sergio Moreno[1]

Instituto de Microbiología Bioquímica, Departamento de Microbiología y Genética, CSIC/Universidad de Salamanca, Edificio Departamental, Campus Miguel de Unamuno, 37007 Salamanca, Spain

[1]Corresponding author
e-mail: smo@gugu.usal.es

In fission yeast, the cyclin-dependent kinase (CDK) inhibitor $p25^{rum1}$ is a key regulator of progression through the G_1 phase of the cell cycle. We show here that $p25^{rum1}$ protein levels are sharply periodic. $p25^{rum1}$ begins to accumulate at anaphase, persists in G_1 and is destroyed during S phase. $p25^{rum1}$ is stabilized and polyubiquitinated in a mutant defective in the 26S proteasome, suggesting that its degradation normally occurs through the ubiquitin-dependent 26S proteasome pathway. Phosphorylation of $p25^{rum1}$ by cdc2–cyclin complexes at residues T58 and T62 is important to target the protein for degradation. Mutation of one or both of these residues to alanine causes stabilization of $p25^{rum1}$ and induces a cell cycle delay in G_1 and polyploidization due to occasional re-initiation of DNA replication before mitosis. The CDK–cyclin complex cdc2–cig1, which is insensitive to $p25^{rum1}$ inhibition, seems to be the main kinase that phosphorylates $p25^{rum1}$. Phosphorylation of $p25^{rum1}$ in S phase and G_2 serves as the trigger for $p25^{rum1}$ proteolysis. Thus, periodic accumulation and degradation of the CDK inhibitor $p25^{rum1}$ in G_1 plays a role in setting a threshold of cyclin levels important in determining the length of the pre-Start G_1 phase and in ensuring the correct order of cell cycle events.

Keywords: CDK inhibitor/cyclin/phosphorylation/proteolysis/rum1

Introduction

Eukaryotic cells co-ordinate cell growth with cell division at a point late in G_1 called Start in yeast and the restriction point in animal cells. Beyond this point, cells become committed to a new round of cell division (Hartwell *et al.*, 1974; Pardee, 1974; Nurse, 1975). Genetic analysis in budding and fission yeast identified a single gene, *CDC28*/*cdc2*$^+$, encoding the essential cyclin-dependent kinase (CDK) required not only for passage through Start but also to initiate mitosis (Nurse and Bisset, 1981; Piggott *et al.*, 1982; Reed and Wittenberg, 1990). In the budding yeast *Saccharomyces cerevisiae*, nine different cyclins associate with Cdc28 (Nasmyth, 1993, 1996). Six B-type cyclins (Clb1–6) are required for S phase and mitosis and three G_1 cyclins (Cln1–3) are necessary for passage through Start. The three G_1 cyclins have different functions. Cln3 is needed to promote the activation of Start-dependent transcription factors (SBF and MBF), whereas Cln1 and Cln2 are required to trigger Start-regulated events such as acquisition of pheromone resistance, budding and spindle pole body duplication (Dirick *et al.*, 1995; Stuart and Wittenberg, 1995). In the fission yeast *Schizosaccharomyces pombe*, four cyclins, puc1, cig1, cig2 and cdc13, can form complexes with cdc2 (reviewed in Fisher and Nurse, 1995). cig1, cig2 and cdc13 are B-type cyclins that have been shown to play a role in regulating the cell cycle. cig2 regulates the G_1–S transition (Obara-Ishihara and Okayama, 1994; Martín-Castellanos *et al.*, 1996; Monderset *et al.*, 1996), while cdc13 is the mitotic cyclin (Booher *et al.*, 1989; Moreno *et al.*, 1989). cig1 has been argued to make a minor contribution to the onset of S phase, because cells deleted for *cig2*$^+$ and *cdc13*$^+$ can still undergo S phase but a triple deletion *cig1*Δ *cig2*Δ *cdc13*Δ blocks the cell cycle before the initiation of DNA replication (Fisher and Nurse, 1996; Monderset *et al.*, 1996). The role of puc1 in the fission yeast mitotic cycle has not been clearly established (Forsburg and Nurse, 1991, 1994).

CDK inhibitors are negative regulators of CDK–cyclin complexes. Some CDK inhibitors, like budding yeast Far1, seem to respond to extracellular signals such as the presence of mating pheromones (Chang and Herskowitz, 1990; Peter *et al.*, 1993; Peter and Herskowitz, 1994), but others, like budding yeast $p40^{SIC1}$ (Donovan *et al.*, 1994; Nugroho and Mendenhall, 1994; Schwob *et al.*, 1994; Schneider *et al.*, 1996) or fission yeast $p25^{rum1}$ (Moreno and Nurse, 1994), appear to be part of the intrinsic cell cycle machinery. While Far1 inhibits Cln-type cyclins, $p40^{SIC1}$ and $p25^{rum1}$ are specific inhibitors of B-type cyclins. $p25^{rum1}$ inhibits the cdc2–cdc13 complex, preventing the activation of this mitotic complex in G_1 cells (Correa-Bordes and Nurse, 1995; Martín-Castellanos *et al.*, 1996). $p25^{rum1}$ is also an inhibitor of cig2-associated cdc2 kinase (Correa-Bordes and Nurse, 1995; Martín-Castellanos *et al.*, 1996). It has been proposed that a transient inhibition of cdc2–cig2 complexes in G_1 is important in setting the minimum cell size required to pass Start (Labib and Moreno, 1996; Martín-Castellanos *et al.*, 1996). Thus, $p25^{rum1}$ plays a central role in the regulation of the fission yeast G_1 phase. It prevents the onset of mitosis in cells that have not initiated DNA replication and it determines the cell cycle timing of Start, maintaining cells in the pre-Start state until they have attained the minimal critical mass required to initiate the cell cycle.

Degradation of cyclins and CDK inhibitors is important for moving from one phase of the cell cycle to the next (reviewed by Deshaies, 1995). Degradation of mitotic cyclins depends on a sequence located near the amino-terminus called the destruction box, which targets cyclins

to the ubiquitin-dependent proteolytic pathway (Glotzer *et al.*, 1991; Hershko *et al.*, 1991). A multiprotein complex, called cyclosome or anaphase-promoting complex (APC), has been shown to contain the E3 ubiquitin–protein ligase activity that catalyses the ligation of multiple ubiquitin molecules to cyclins (Hershko *et al.*, 1994; King *et al.*, 1995; Sudakin *et al.*, 1995). APC is a high molecular weight complex that contains the Cdc16, Cdc23 and Cdc27 protein members of the TPR family essential for the onset of anaphase (Irniger *et al.*, 1995; Tugendreich *et al.*, 1995), highly conserved among eukaryotes (Hirano *et al.*, 1988; O′Donnell *et al.*, 1991; Mirabito and Morris, 1993; Samejima and Yanagida, 1994; King *et al.*, 1995; Tugendreich *et al.*, 1995). The fission yeast cut2 protein (a protein that might be involved in holding sister chromatids together until the onset of anaphase) also contains a destruction box that is recognized by APC in mitosis and destroyed through this proteolytic pathway (Funabiki *et al.*, 1996). Degradation of the mitotic cyclins occurs in an interval from anaphase until passage through Start or the restriction point in late G_1 (Amon *et al.*, 1994; Brandeis and Hunt, 1996). This prevents the accumulation of mitotic cyclins before the formation of the G_1 complexes, and this period of low CDK activity is thought to be important for proper assembly of pre-initiation DNA replication complexes (Adachi and Laemmli, 1994; Dahmann *et al.*, 1995; Nasmyth, 1996; Stern and Nurse, 1996; Wuarin and Nurse, 1996).

During the G_1 phase, the right balance of cyclins and CDK inhibitors is necessary to produce a co-ordinate Start to the cell cycle. In budding yeast, G_1 cyclins have very short half-lives and are destroyed as cells enter S phase. Degradation of the CDK inhibitor $p40^{SIC1}$ is required for cells to initiate S phase (Schwob *et al.*, 1994; Schneider *et al.*, 1996). Proteolysis of G_1 cyclins and of $p40^{SIC1}$ also occurs through the ubiquitin-dependent proteolytic pathway and requires the participation of a ubiquitin–protein ligase complex, different from APC, formed by a multiprotein complex containing the product of the *CDC34*, *CDC4*, *SKP1* and *CDC53* genes (Schwob *et al.*, 1994; Deshaies, 1995; Bai *et al.*, 1996; Connelly and Hieter, 1996; Schneider *et al.*, 1996; Willems *et al.*, 1996; Verma *et al.*, 1997). *CDC34* encodes an E2 ubiquitin-conjugating enzyme (Goebl *et al.*, 1988), *CDC4* a protein with WD40 repeats (Yochem and Byers, 1987), *SKP1* a protein that interacts with Cdc4 (Bai *et al.*, 1996; Connelly and Hieter, 1996) and *CDC53* a member of the cullin protein family conserved in yeast, *Caenorhabditis elegans*, *Drosophila* and humans (Kipreos *et al.*, 1996; Mathias *et al.*, 1996). Mutations in any of these genes lead to stabilization of $p40^{SIC1}$ and G_1 cyclins. G_1 cyclins are unstable because they contain PEST sequences (Rogers *et al.*, 1986). CDK phosphorylation of residues located near the PEST sequence seems to be the signal that targets Cln2 and Cln3 to degradation (Yaglom *et al.*, 1995; Lanker *et al.*, 1996).

CDK–cyclin complexes not only play positive roles in the cell cycle, determining when cells initiate S phase or mitosis, but are also required to inhibit the initiation of a unscheduled cell cycle event. In fission yeast, inactivation of the mitotic cdc2–cdc13 complex causes cells to undergo repeated rounds of DNA replication without intervening mitoses (Broek *et al.*, 1991; Hayles *et al.*, 1994; Fisher and Nurse, 1996). Budding yeast mutants with low levels of Cdc28–Clb5 kinase re-replicate (Dahmann *et al.*, 1996), *Drosophila* mutants in cyclin A also undergo re-replication (Sauer *et al.*, 1995) and, in starfish oocytes, cyclin B suppresses DNA replication between meiosis I and meiosis II (Adachi and Laemmli, 1994; Picard *et al.*, 1996). These results suggest that CDK–cyclin complexes play a dual role in the cell cycle. They are required to promote the initiation of S phase and mitosis and, in addition, in G_2 they prevent extra rounds of DNA replication within the same cell cycle (Nurse, 1994; Nasmyth, 1996; Stern and Nurse, 1996). In fission yeast, high level expression of the *rum1*$^+$ gene blocks mitosis but allows repeated rounds of DNA replication (Moreno and Nurse, 1994). This result is explained because $p25^{rum1}$ strongly inhibits the cdc2–cdc13 complex leading to a phenotype which is similar to the *cdc13*$^+$ deletion (Hayles *et al.*, 1994). Thus, transit from G_2 to G_1 in fission yeast occurs by inactivation of the cdc2–cdc13 kinase complex, either by destruction of the mitotic cdc13 cyclin in mitosis, or by production of high levels of the $p25^{rum1}$ CDK inhibitor. According to this idea, the presence of cdc2–cdc13 activity defines a cell in G_2, and destruction of this complex in mitosis resets the cell to G_1, allowing a new S phase (Nurse, 1994; Stern and Nurse, 1996). Therefore, G_1 is defined as a period of low CDK–cyclin activity prior to the initiation of a new cell cycle.

Here we have studied the regulation of the $p25^{rum1}$ protein. We have found that $p25^{rum1}$ levels sharply oscillate during the fission yeast cell cycle. This oscillation is due mainly to changes in protein stability. $p25^{rum1}$ is stabilized in G_1, a period were there is low CDK–cyclin activity, and is destroyed as cells enter S phase, when CDK–cyclin activity begins to rise. We have also found that phosphorylation of $p25^{rum1}$ by cdc2–cyclin complexes at the end of G_1 is important for targeting $p25^{rum1}$ for degradation.

Results

p25^{rum1} level oscillates through the cell cycle

In order to study the regulation of the *rum1*$^+$ gene through the cell cycle, we determined the levels of $p25^{rum1}$ and of *rum1*$^+$ mRNA in synchronous cultures. Rapidly growing wild-type fission yeast cells have a very short G_1 and lack the pre-Start G_1 interval. Since *rum1*$^+$ function is required in G_1, we used the temperature-sensitive mutant *wee1-50* where the pre-Start G_1 interval is extended when incubated at the restrictive temperature of 36°C (Nurse, 1975) (Figure 1A). Cells of the *wee1-50* strain were grown at 25°C, and a synchronous culture was made using an elutriator rotor. Small cells in early G_2 were selected and incubated at 36°C. These cells proceeded synchronously into mitosis. Cell cycle position and the degree of synchrony were monitored by determining the mitotic index and the percentage of cells in G_1 after flow cytometry analysis, as a function of time. Protein extracts were prepared every 20 min for two cell cycles, and $p25^{rum1}$ levels were measured by Western blotting using an anti-$p25^{rum1}$ affinity-purified polyclonal antibody. $p25^{rum1}$ levels were sharply periodic, rising to a peak 40 min after the shift as cells were undergoing anaphase and decreasing at 100 min when the cells where exiting G_1 (Figure 1B). In

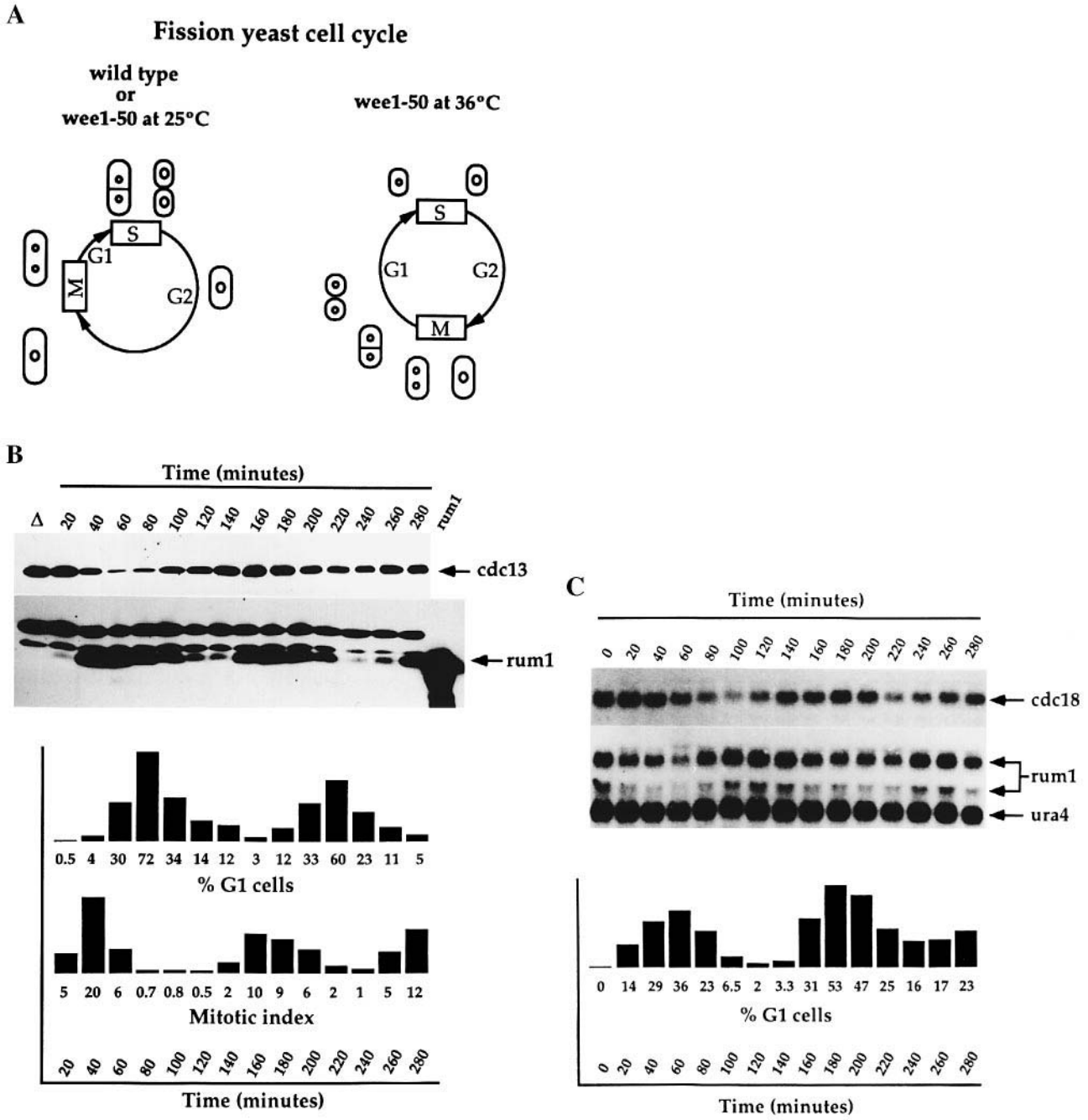

Fig. 1. Periodicity of $p25^{rum1}$ and *rum1*$^+$ mRNA levels during the cell cycle. $p25^{rum1}$ protein and *rum1*$^+$ mRNA levels were measured in a synchronous culture of the temperature-sensitive *wee1-50* strain. (**A**) Wild-type or *wee1-50* cells at 25°C have a very short G_1. *wee1-50* cells at 36°C enter mitosis with a reduced cell size and, as a consequence, they have an extended G_1 to meet the minimal cell size requirement to pass Start. (**B**) A homogeneous population of cells in early G_2 was selected by elutriation of the *wee1-50* strain at 25°C. This culture was incubated for 20 min at 25°C and then shifted up to 36°C. Samples were taken every 20 min to determine cdc13 and rum1 protein levels, the percentage of G_1 cells and the mitotic index. rum1 and cdc13 protein levels were measured by Western blot using affinity-purified R3 anti-rum1 polyclonal antibody and affinity-purified SP4 anti-cdc13 polyclonal antibody, respectively. The percentage of G_1 cells was measured by flow cytometry and the mitotic index by counting the number of cells in anaphase after DAPI staining (see Materials and methods). $p25^{rum1}$ levels increase as cells undergo anaphase and decrease as cells enter S-phase. In contrast, levels of cdc13 decrease in anaphase and increase at the end of G_1. We used a *rum1*Δ (Δ) and purified $p25^{rum1}$ (rum1) as negative and positive controls. (**C**) *rum1*$^+$ mRNA levels determined in a similar experiment also oscillate during the cell cycle. The time of the peak of transcription was 40 min earlier than the time of the peak of the protein. We observed a 10-fold oscillation in the levels of protein compared with a 2- to 3-fold in the level of the transcript. The blot was probed with *ura4*$^+$ as a loading control and with *cdc18*$^+$ as a gene known to be transcribed in G_1/S (Kelly *et al.*, 1993). *rum1*$^+$ mRNA levels were normalized using the *ura4*$^+$ gene.

the same experiment, $p56^{cdc13}$ levels were exactly the opposite to those of $p25^{rum1}$. $p56^{cdc13}$ levels dropped at the onset of anaphase and started to accumulate during the next S phase. This experiment shows that $p25^{rum1}$ protein levels oscillate though the cell cycle and that the levels are maximal in G_1, consistent with previous observations where $p25^{rum1}$ was shown to accumulate in cells arrested in G_1 but not in S phase or G_2 (Correa-

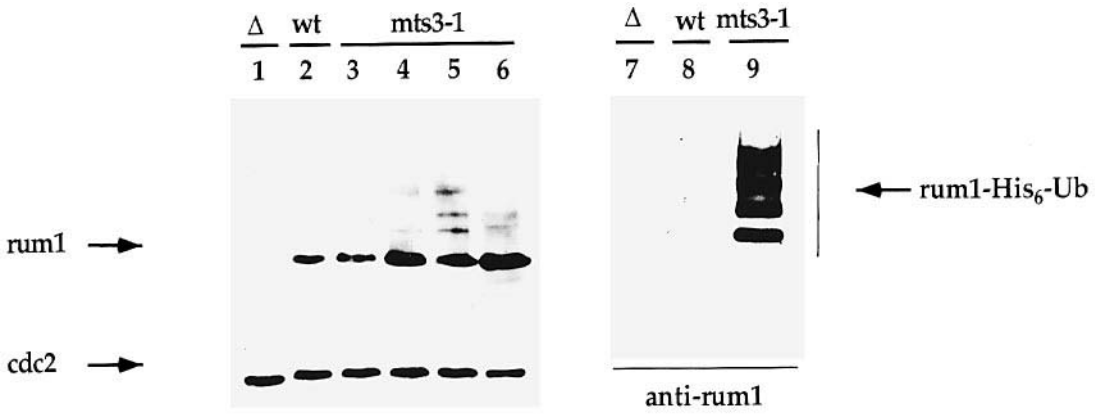

Fig. 2. $p25^{rum1}$ is stabilized in the *mts3-1* mutant defective in subunit 14 of the 26S proteasome. Cells of the *rum1*$^+$ deletion (Δ, lane 1) wild-type (wt, lane 2) and the temperature-sensitive *mts3-1* mutant (mts3-1, lanes 3–6) were grown at 25°C and shifted to 36°C for 6 h. Samples were taken at 0, 2, 4 and 6 h after the shift, and levels of $p25^{rum1}$ and $p34^{cdc2}$, as a loading control, were determined by Western blot using affinity-purified R4 anti-rum1 and PN24 anti-cdc2 antibodies. His_6-ubiquitin was expressed from the *nmt1* promoter for 22 h at 25°C and then shifted to 36°C for a further 4 h in the *rum1*$^+$ deletion (Δ, lane 7), wild-type (wt, lane 8) and in the *mts3-1* mutant cells (mts3-1, lane 9). The His_6-ubiquitin conjugates were purified on Ni^{2+}-NTA columns and analysed by Western blot using affinity-purified R4 anti-rum1 antibody (1:50).

Bordes and Nurse, 1995). *rum1*$^+$ mRNA levels were also determined in a similar experiment and found to oscillate through the cell cycle with a peak of expression at the end of the G_2 phase, 40–60 min earlier than the protein (Figure 1C). Levels of *rum1*$^+$ mRNA only changed 2- to 3-fold (when normalized to the *ura4*$^+$ mRNA) compared with a 10-fold oscillation in the protein levels, suggesting that additional post-transcriptional mechanisms are involved in regulating $p25^{rum1}$ levels.

$p25^{rum1}$ is polyubiquitinated and degraded by the proteasome pathway

Protein degradation plays a crucial role in the regulation of the cell cycle. Destruction of mitotic cyclins controls exit from mitosis into G_1 (Murray and Kirschner, 1989; Murray *et al.*, 1989). In the budding yeast and animal cells, G_1 cyclins and the CDK inhibitors $p40^{SIC1}$ and $p27^{KIP1}$ are destroyed at the end of G_1 by the ubiquitin-dependent proteasome pathway (Wittenberg *et al.*, 1990; Tyers *et al.*, 1992; Donovan *et al.*, 1994; Schwob *et al.*, 1994; Deshaies *et al.*, 1995; Pagano *et al.*, 1995; Bai *et al.*, 1996; Clurman *et al.*, 1996; Willems *et al.*, 1996; Won and Reed, 1996; Diehl *et al.*, 1997). To establish whether $p25^{rum1}$ is a substrate of the proteasome degradation pathway, we determined $p25^{rum1}$ levels in the fission yeast temperature-sensitive mutant *mts3-1*, defective in subunit 14 of the 26S proteasome (Gordon *et al.*, 1996). $p25^{rum1}$ levels were measured in this mutant at 25°C and 2, 4 and 6 h after the shift to 36°C. $p25^{rum1}$ protein was more abundant in the *mts3-1* mutant at the restrictive temperature than in the wild-type strain (Figure 2, lanes 1–6), suggesting that the proteasome degradation pathway is involved in regulating $p25^{rum1}$ levels. In this experiment, we used affinity-purified R4 rum1 antibody that reacts with a single band in wild-type cells. This antibody recognized several high molecular weight bands in the *mts3-1* mutant at 36°C that could be $p25^{rum1}$ ubiquitin conjugates (Figure 2, lanes 4, 5 and 6). To investigate this possibility, we expressed in fission yeast a His_6-tagged version of ubiquitin. Extracts from the *rum1* deletion, the wild-type and the *mts3-1* mutant expressing His_6-ubiquitin were purified using Ni^{2+}-NTA resin (Treier *et al.*, 1994), separated on a polyacrylamide gel and then Western blotted with anti-rum1 R4 antibody. Reactive high molecular weight bands were detected in the *mts3-1* mutant expressing His_6-ubiquitin at the restrictive temperature (Figure 2, lane 9). These bands were absent both in wild-type and *rum1*$^+$-deleted cells expressing His_6-ubiquitin grown under identical conditions (Figure 2, lanes 7 and 8). This result clearly shows that $p25^{rum1}$ is polyubiquitinated and degraded through the ubiquitin-dependent 26S proteasome pathway.

Phosphorylation of $p25^{rum1}$ is important for its stability

In budding yeast, phosphorylation of several Cdc28-specific sites in the carboxy-terminus of the G_1 cyclins Cln2 and Cln3 is important in promoting their degradation (Yaglom *et al.*, 1995; Lanker *et al.*, 1996). We have found in $p25^{rum1}$ eight putative CDK phosphorylation sites containing the minimal consensus sequence of S/T·P (Figure 3A). Three of these sites, at positions 58, 62 and 212, correspond exactly to the full consensus cdc2 phosphorylation site of S/T·P·X·K/R (where X is any amino acid) (Moreno and Nurse, 1990). We have mutated all eight serines and threonines to alanine and expressed each mutant using the *nmt1* promoter in *S.pombe*. Mutants *rum1-A58* and *rum1-A62* showed a phenotype consistent with hyperactivation or stabilization of $p25^{rum1}$. In both cases, very few transformants were obtained even when we used the weakest modified *nmt1* promoter (pREP81X) to transform yeast cells in the presence of thiamine, compared with a control pREP3X plasmid with the *rum1*$^+$ gene (data not shown, see below). The transformants grew very slowly into small colonies containing many elongated cells with a phenotype similar to the phenotype of cells overexpressing the wild-type *rum1*$^+$ gene (Moreno and Nurse, 1994). A double mutant *rum1-A58A62* showed a more severe phenotype than each of the single mutants. Cells transformed with the rest of the alanine mutants (A5, A13A16A19, A110 and A212) showed a phenotype identical to cells expressing wild-type *rum1*$^+$ plasmid control (data not shown).

Expression of the *rum1*$^+$ gene driven by its own

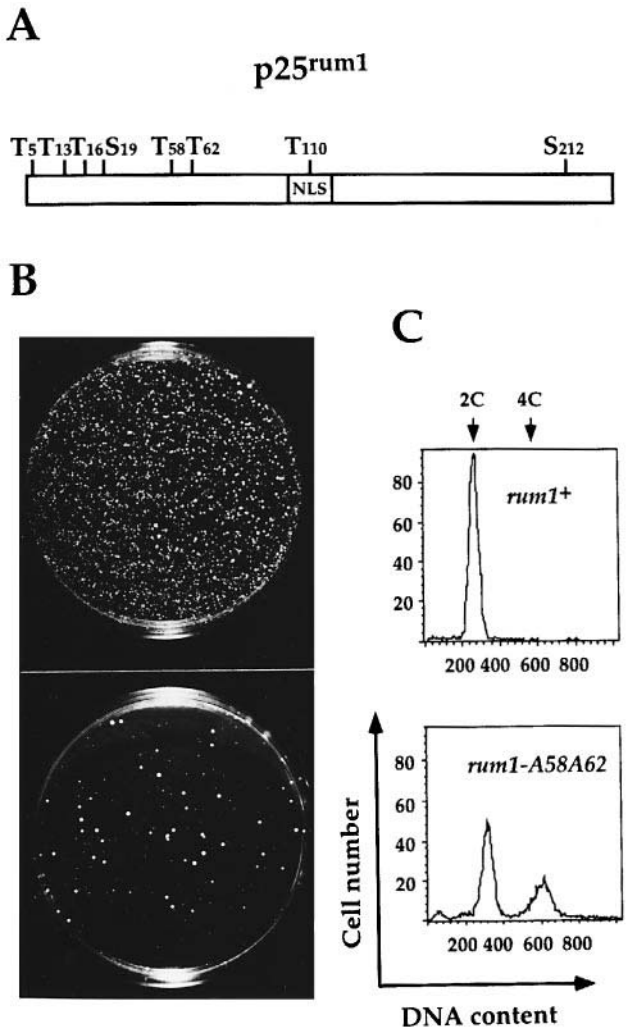

Fig. 3. *rum1*$^+$ mutants in two putative CDK phosphorylation sites, T58 and T62, show a phenotype consistent with a hyperactivation or stabilization of p25^{rum1}. (**A**) Schematic representation of p25^{rum1} showing eight serine or threonine residues that occur in S/T·P sequences. T58, T62 and S212 are contained in the sequence S/T·P·X·K/R, a full CDK phosphorylation consensus site. Each of these residues was mutated to alanine. Single mutants in residues T58 and T62 showed a gain-of-function phenotype consistent with the mutant protein being either a better inhibitor or more stable than the wild-type protein. NLS, nuclear localization sequence. (**B**) Transformation of pIRT2-*rum1*$^+$ (top panel) and pIRT2-*rum1-A58A62* (bottom panel) into a *rum1*Δ *leu1-32* strain. (**C**) Flow cytometric analysis of wild-type and *rum1-A58A62* integrant strains growing exponentially in minimal media.

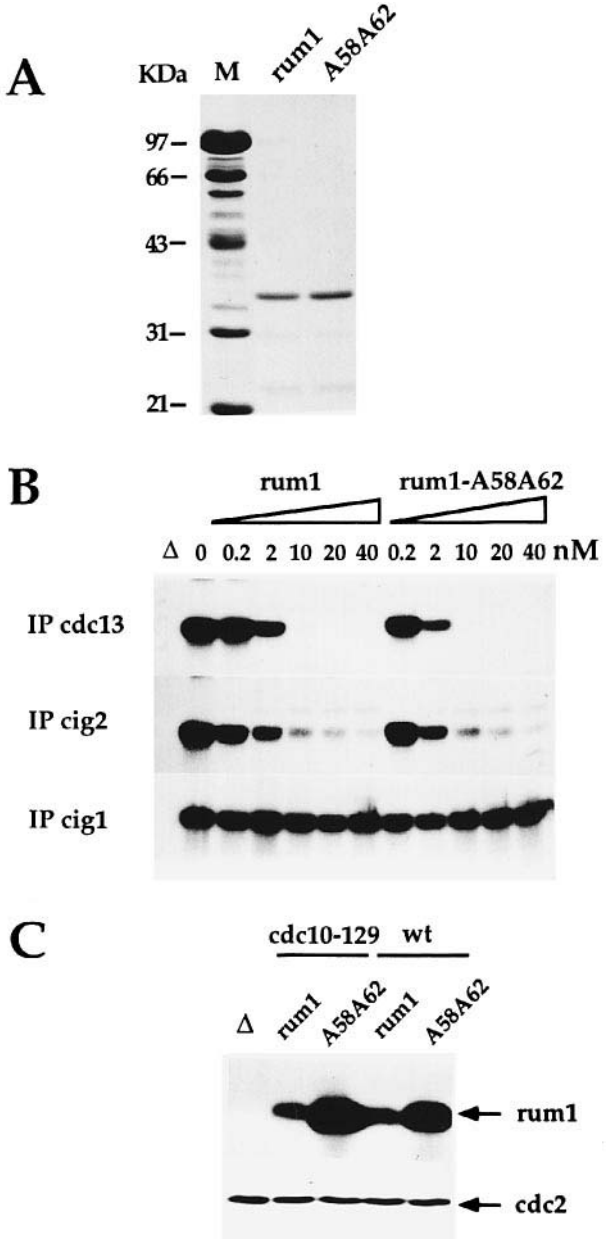

Fig. 4. p25$^{rum1\text{-}A58A62}$ has the same activity as a CDK inhibitor but is more stable than p25^{rum1}. (**A**) Coomassie blue-stained SDS–PAGE of purified p25^{rum1} and p25$^{rum1\text{-}A58A62}$. Both proteins migrated with an M_r of 34 kDa. (**B**) Wild-type fission yeast extracts were immunoprecipitated with anti-cdc13, anti-cig2 and anti-cig1 antibodies. The immunoprecipitates were pre-incubated with different concentrations of either p25^{rum1} or p25$^{rum1\text{-}A58A62}$ and then assayed for histone H1 kinase activity. As negative controls (Δ), extracts of *cig1*Δ and *cig2*Δ were immunoprecipitated with anti-cig1 and anti-cig2 antibodies and assayed for H1 kinase activity. (**C**) Western blot of exponentially growing *rum1*Δ, *cdc10–129 rum1*Δ *int::rum1*$^+$, *cdc10-129 rum1*Δ *int::rum1-A58A62*, *rum1*Δ *int::rum1*$^+$ and *rum1*Δ *int::rum1-A58A62*. Levels of p25^{rum1} and p34^{cdc2}, as a loading control, were determined by Western blot of total extracts (100 μg) using affinity-purified R4 anti-rum1 and PN24 anti-cdc2 antibodies.

promoter using the multicopy plasmid pIRT2 gives a fully wild-type phenotype, with no signs of cell elongation or diploidization. When we expressed the *rum1-A58A62* mutant allele driven by the *rum1*$^+$ promoter using the pIRT2 plasmid, we obtained many small microcolonies and a few normal size colonies, all of which were integrants (Figure 3B). Flow cytometry analysis of these integrants showed a high frequency of diploids (Figure 3C).

The phenotype of the cells expressing the *rum1-A58A62* mutant could be explained either because the mutant protein is more active as a CDK inhibitor or because it is more stable, or both. To distinguish between these possibilities, we expressed wild-type *rum1*$^+$ and mutant *rum1-A58A62* in *Escherichia coli* and purified both proteins to homogeneity as judged by Coomassie blue staining (Figure 4A). Different amounts of purified p25^{rum1} and p25$^{rum1\text{-}A58A62}$ were added to cdc13, cig2 and cig1 immunoprecipitates, and protein kinase activity was assayed using histone H1 as a substrate (Figure 4B). Both p25^{rum1} and p25$^{rum1\text{-}A58A62}$ were able to inhibit the cdc13- and the

cig2-associated H1 kinase activity to the same extent, indicating that at least *in vitro* there is no difference in the activity of these two proteins. In contrast, cdc2–cig1 kinase activity was not significantly inhibited by either $p25^{rum1}$ or by $p25^{rum1\text{-}A58A62}$ (Figure 4B), suggesting that this complex is insensitive to $p25^{rum1}$ inhibition.

As $p25^{rum1}$ and $p25^{rum1\text{-}A58A62}$ behave similarly as CDK inhibitors, a possible explanation for the phenotype of the *rum1-A58A62* integrants is that the two proteins have different stabilities *in vivo*. We have compared $p25^{rum1}$ levels in single copy integrants of *rum1*$^+$ and *rum1-A58A62* obtained in a *rum1*Δ background strain. Steady-state levels of $p25^{rum1\text{-}A58A62}$ were at least 4-fold higher than wild-type $p25^{rum1}$ levels (Figure 4C), indicating that the more likely explanation for the phenotypes associated with the *rum1-A58A62* mutant allele is that the mutant protein is more stable *in vivo* than the wild-type protein.

Stabilization of $p25^{rum1}$ causes a cell cycle delay in G_1

To confirm this hypothesis, we studied the stability of $p25^{rum1}$ and $p25^{rum1\text{-}A58A62}$ proteins through the cell cycle using the *cdc10-129* mutant to synchronize cells in G_1. This was investigated by integrating the wild-type *rum1*$^+$ gene and the *rum1-A58A62* mutant allele in a *cdc10-129 rum1*Δ strain. Exponentially growing cultures of *cdc10-129 rum1*Δ *int-rum1*$^+$ and *cdc10-129 rum1*Δ *int-rum1-A58A62* were incubated for 4 h at 36°C and then released to 25°C. Wild-type $p25^{rum1}$ disappeared by 90 min after the release as cells were entering S phase (Figure 5A and C). In contrast, the $p25^{rum1\text{-}A58A62}$ levels were high and stable during the course of the experiment (Figure 5B). These levels of $p25^{rum1\text{-}A58A62}$ were reduced compared with the levels required to block mitosis in cells overproducing *rum1*$^+$ from the *nmt1* promoter (Figure 5B, ovp). Interestingly, the *cdc10-129 rum1*Δ strain with the integrated *rum1-A58A62* allele underwent S phase and mitosis even in the presence of considerable amounts of $p25^{rum1\text{-}A58A62}$ mutant protein (Figure 5B and C). Flow cytometry analysis showed that both strains underwent S phase after the release, though with a delay of ~15 min in the strain containing the *rum1-A58A62* allele (Figure 5C). We also observed a delay of ~30 min in the accumulation of cdc13 cyclin in cells expressing *rum1-A58A62* compared with the control, indicating that once cells initiate DNA replication the cdc13 protein levels increase independently of the presence or absence of $p25^{rum1}$ protein.

If $p25^{rum1}$ plays a role in determining the length of G_1, stabilization of this protein should delay the onset of S phase. Flow cytometry analysis of haploid integrants of the *rum1-A58A62* allele in the *rum1* deletion (*rum1*Δ) and in the *cdc10-129 rum1*Δ strains grown at 25°C clearly revealed a G_1 population (Figure 6A). To quantify this delay, we selected the smallest cells in the *cdc10-129 rum1*Δ *int-rum1-A58A62* culture, that were in G_1, S and early G_2 phases, by elutriation at 25°C. Half of these cells were incubated at 25°C and samples for flow cytometry analysis were taken every 20 min for 6 h (Figure 6B, left). All the G_1 cells underwent S phase by 40 min. In the next cell cycle, these cells remained in G_1 for ~90 min after cytokinesis. Considering that the cell cycle length in this experiment was 260 min, then the

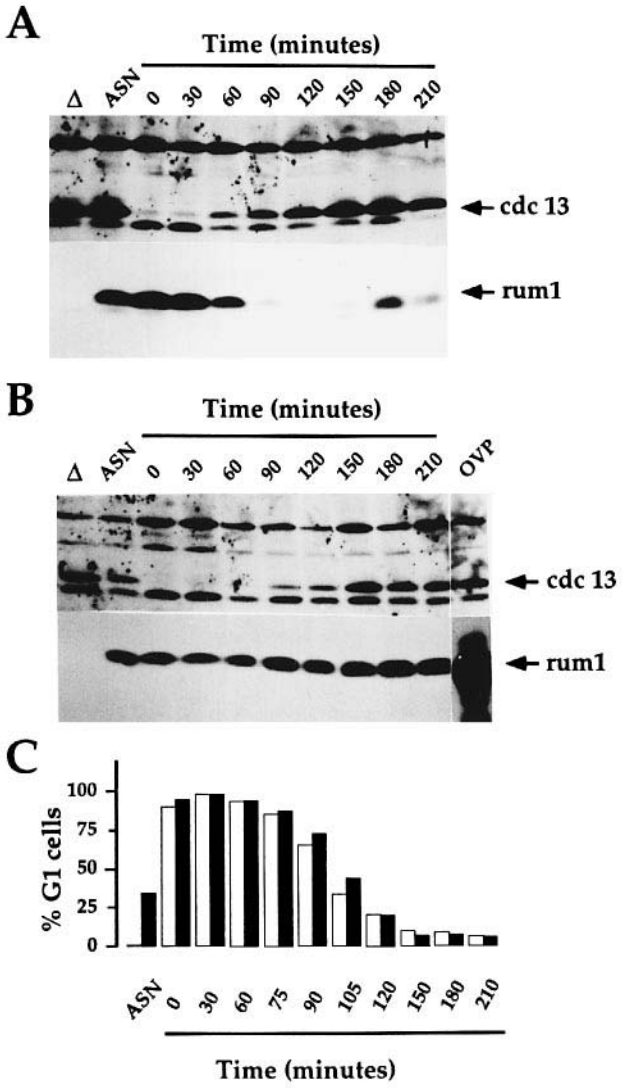

Fig. 5. $p25^{rum1\text{-}A58A62}$ is stable throughout the cell cycle. Cultures of *cdc10-129 rum1*Δ *int::rum1*$^+$ (**A**) and *cdc10-129 rum1*Δ *int::rum1-A58A62* (**B**) were grown at 25°C to mid-exponential phase in minimal medium, shifted to 36°C for 4 h and then released at 25°C. Samples for Western blot and flow cytometry were taken before the shift to 36°C (ASN), 4 h after the shift to 36°C (t = 0) and every 30 min after the release at 25°C. Levels of $p25^{rum1}$ and $p56^{cdc13}$ were determined in both strains. (**A**) $p25^{rum1}$ levels were high at the block point (t = 0) and disappeared just before the onset of S phase (t = 60). (**B**) $p25^{rum1\text{-}A58A62}$ levels were high and constant throughout the experiment. $p56^{cdc13}$ levels were undetectable at the *cdc10-129* arrest point and then increased in both strains as cells underwent S phase. A delay of ~30 min in the accumulation of $p56^{cdc13}$ and in the onset of S phase was observed in the strain expressing *rum1-A58A62* compared with the control strain. *rum1*Δ (Δ) and *rum1*$^+$ overexpressor (OVP) strains were used as negative and positive controls. (**C**) The percentage of cells in G_1 after the release to 25°C. Asn, asynchronous cells grown at 25°C. White bars, *cdc10-129 rum1*Δ *int::rum1*$^+$ cells. Black bars, *cdc10-129 rum1*Δ *int::rum1-A58A62* cells.

onset of S phase was delayed by as much as 0.3 of a cell cycle. In a synchronous culture of the *cdc10-129* control strain at 25°C, we did not observe any delay in G_1 (data not shown, see Moreno and Nurse 1994 Figure 4D). The other half of the cells were shifted at time 0 after elutriation to 36°C. Ninety percent of these cells underwent one complete round of cell division and then arrested at the *cdc10* block point in G_1 (Figure 6B, right). The remaining

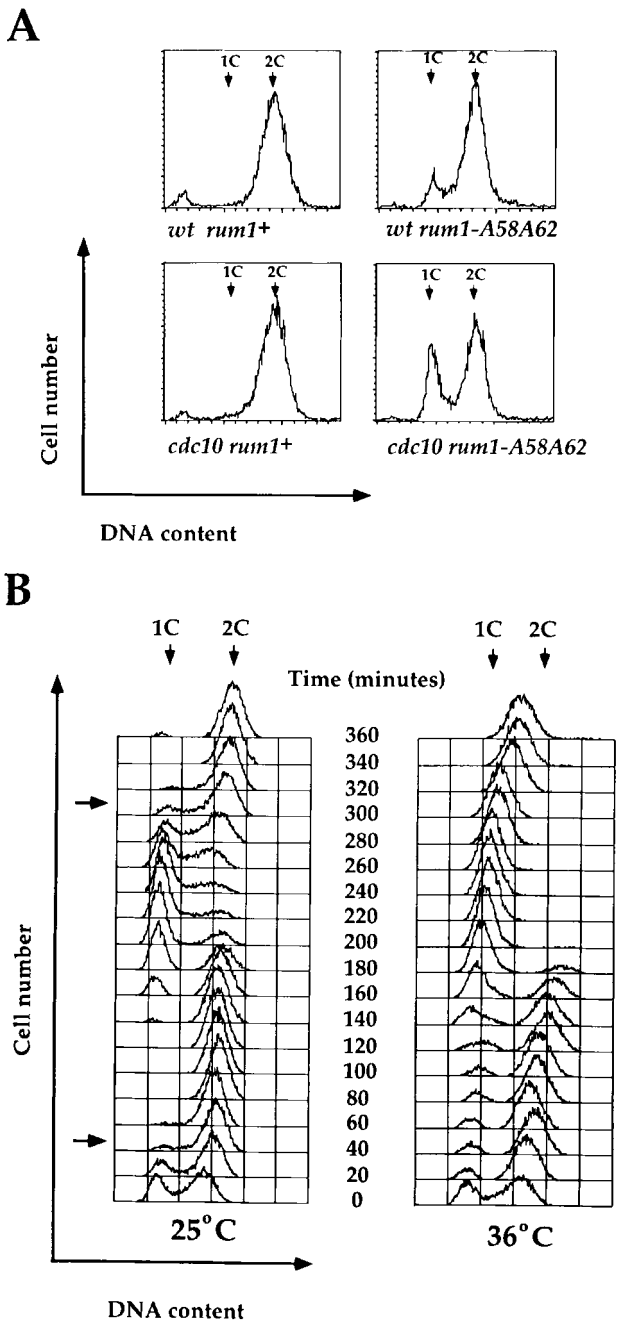

Fig. 6. Expression of *rum1-A58A62* mutant causes a cell cycle delay in G_1. (**A**) Flow cytometry of *rum1Δ int::rum1*$^+$, *rum1Δ int::rum1-A58A62*, *cdc10-129 rum1Δ int::rum1*$^+$and *cdc10-129 rum1Δ int::rum1-A58A62* haploid cells growing exponentially at 25°C in minimal medium. Since expression of *rum1-A58A62* mutant allele induces a high degree of diploidization, for this experiment a fresh haploid pink colony was selected from a YES phloxin B plate and inoculated in minimal medium until early exponential phase. The DNA content was measured by FACS analysis. (**B**) A synchronous culture of the *cdc10-129 rum1Δ int-rum1::A58A62* haploid strain was prepared at 25°C. Half of the culture was incubated at 25°C (left panel) and the other half at 36°C (right panel). The generation time of the cells growing at 25°C was 260 min as determined using the two samples shown with arrows with a similar FACS profile and separated by one generation time. The G_1 delay of 90 min was estimated using the 260 and 170 min samples (in between 160 and 180 min), where ~50% of the cells have 1C and 50% 2C DNA content.

10% stayed in G_1 for the rest of the experiment, indicating that at least some of the cells selected by elutriation were in pre-Start G_1 when the cdc10 function was inactivated by the temperature shift.

p25^{rum1} is phosphorylated in vivo

From the previous experiments, we concluded that mutations in two putative cdc2 phosphorylation sites, T58 and T62, affect the stability of p25^{rum1}. One possible hypothesis is that phosphorylation of p25^{rum1} by cdc2 on residues T58 and/or T62 could target p25^{rum1} for destruction at the end of G_1. We have found that p25^{rum1} protein is an excellent substrate for the cdc2 protein kinase. Phosphorylation of p25^{rum1} *in vitro* by immunocomplexes of cdc2 induced a mobility shift from 34 to 36 kDa (Figure 7A). This shift in mobility was not observed when we used the mutant p25$^{rum1\text{-}A58A62}$ as a substrate, suggesting that at least *in vitro* cdc2 was able to phosphorylate p25^{rum1} on residues T58 and T62. We next studied which of the cdc2 complexes were involved in this phosphorylation event. Immunoprecipitates of cdc13, cig2 and cig1 were assayed using p25^{rum1}, p25$^{rum1\text{-}A58A62}$ and histone H1 as substrates. We found that cdc2–cig1 complexes were able to phosphorylate p25^{rum1} as efficiently as histone H1 and to induce a mobility shift in p25^{rum1} similar to the one induced by immunocomplexes of cdc2 (Figure 7A). Phosphorylation of p25^{rum1} by cdc2–cig2 and cdc2–cdc13 was detected only after very long exposures and seemed to occur at sites other than T58 and T62 (Figure 7A, see figure legend). Furthermore, immunocomplexes of cdc2 from cells deleted for *cig1*$^+$ gave a pattern of p25^{rum1} phosphorylation very similar to the one induced by cdc2–cig2 and cdc2–cdc13 (Figure 7A). This result suggests that cdc2–cig1 complexes, which are insensitive to p25^{rum1} inhibition (Figure 4B; Correa-Bordes and Nurse, 1995; Martín-Castellanos *et al.*, 1996), are involved in the phosphorylation of p25^{rum1}.

To determine if p25^{rum1} is phosphorylated *in vivo*, we immunoprecipitated p25^{rum1} from ^{32}P-labelled cells. A faint 36 kDa band was detected from wild-type cells (Figure 7B, left panel). This band was absent in the *rum1Δ* and appeared much stronger in cells overproducing *rum1*$^+$ (Figure 7B, left panel), suggesting that it should correspond to *in vivo* labelled p25^{rum1}. Given that phosphorylation of p25^{rum1} seems to be the signal that triggers its degradation, it is expected that the half-life of phosphorylated p25^{rum1} would be very short. Hence we have to overexpress the protein to moderate levels to be able to obtain enough labelled protein to make the phosphopeptide maps. We used single copy integrants of wild-type *rum1*$^+$ or the *rum1-A58A62* mutant allele expressed from the weakest version of the *nmt1* promoter (pREP81X). In these conditions, we found a 5-fold reduction in the phosphorylation of mutant p25$^{rum1\text{-}A58A62}$ as compared with wild-type p25^{rum1} (Figure 7B, right panel; Figure 8A). In addition, there was a clear mobility shift in the phosphorylated wild-type p25^{rum1} compared with the mutant protein (Figure 7B, right panel; Figure 8A). The apparent size of *in vivo* phosphorylated p25^{rum1} was 2 kDa larger than p25$^{rum1\text{-}A58A62}$, indicating that phosphorylation of p25^{rum1} *in vivo* was causing a shift in mobility identical to the one observed when p25^{rum1} was phosphorylated *in vitro*

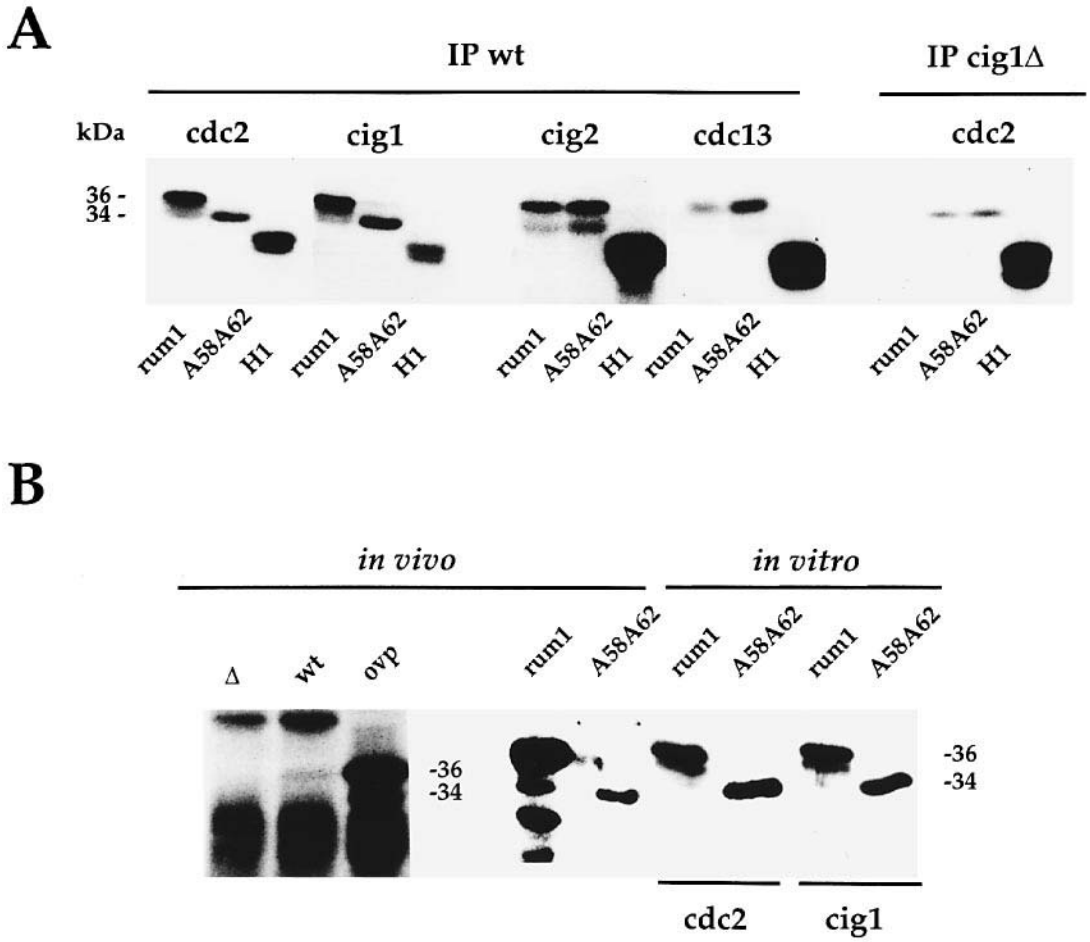

Fig. 7. p25^{rum1} is phosphorylated *in vivo*. (**A**) Wild-type and *cig1*-deleted cells were grown to mid-exponential phase in minimal medium. Extracts were prepared in HB buffer (see Materials and methods) and 2 mg of total protein was immunoprecipitated with anti-cdc2, anti-cig1, anti-cig2 and anti-cdc13 antibodies. Protein kinase activity was measured using p25^{rum1} (rum1), p25$^{rum1\text{-}A58A62}$ (A58A62) and histone H1 (H1) as substrates. The phosphorylated products were separated in a long run 14% SDS–PAGE and exposed to autoradiography. cdc2 immunocomplexes could phosphorylate p25^{rum1} as efficiently as they could histone H1. p25^{rum1} phosphorylation induced a band shift from 34 to 36 kDa that was not observed in the mutant p25$^{rum1\text{-}A58A62}$. cig1 immunocomplexes induced a similar band shift to cdc2. p25^{rum1} was a much poorer substrate than histone H1 for the cig2 and cdc13 immunocomplexes. The cdc2 and cig1 gels were exposed for 8 h and the cig2 and cdc13 gels for 40 h. (**B**) Extracts from *rum1*$^{+}$-deleted cells (Δ), wild-type (wt) and cells overproducing *rum1*$^{+}$ (ovp) labelled *in vivo* with [^{32}P]orthophosphate were immunoprecipitated with R4 anti-rum1 antibody and separated on an SDS–PAGE gel. Coomassie blue staining of purified p25^{rum1} was used as the 34 kDa molecular weight marker. Cells expressing *rum1*$^{+}$ or *rum1-A58A62* from the weakest version of the *nmt1* promoter (pREP81X) were labelled *in vivo* and immunoprecipitated with R4 anti-rum1 antibody (*in vivo* rum1, A58A62) and run on a long SDS–PAGE gel together with p25^{rum1} and p25$^{rum1\text{-}A58A62}$ phosphorylated *in vitro* with cdc2 or cig1 immunocomplexes (*in vitro* rum1, A58A62). Similar shifts in mobility were seen in p25^{rum1} phosphorylated *in vivo* and *in vitro*.

by cdc2 or cig1 immunocomplexes (Figure 7B, right panel; Figure 8A).

Tryptic phosphopeptide maps of *in vivo* ^{32}P-labelled wild-type p25^{rum1} showed two phosphopeptides (Figure 8B, phosphopeptides 1 and 2), while p25$^{rum1\text{-}A58A62}$ showed only one (corresponding to phosphopeptide 2). Phosphopeptide 1, the major phosphopeptide present in wild-type p25^{rum1}, was absent in the mutant p25$^{rum1\text{-}A58A62}$, suggesting that this phosphopeptide might contain the residues T58 and T62. To confirm this, we performed two experiments. First, phosphoamino acid analysis of phosphopeptide 1 revealed phosphothreonine while phosphopeptide 2 contained phosphoserine. Second, we generated a *rum1-S58S62* mutant allele where the two threonine residues (T58 and T62) were mutated to serine. *In vivo* ^{32}P-labelled p25$^{rum1\text{-}S58S62}$ also showed a shift in mobility similar to wild-type p25^{rum1} (Figure 8A). Tryptic phosphopeptide maps of *in vivo* ^{32}P-labelled p25$^{rum1\text{-}S58S62}$ also showed two main phosphopeptides with migration similar to phosphopeptides 1 and 2 in wild-type p25^{rum1} (Figure 8B). Phosphoamino acid analysis of phosphopeptide 1 in p25$^{rum1\text{-}S58S62}$ revealed phosphoserine instead of the phosphothreonine in wild-type p25^{rum1}. Taken together, these results clearly show that p25^{rum1} is phosphorylated *in vivo* on residues T58 and T62.

cdc2–cig1 influences the stability of p25^{rum1}

To study the timing of activation of the different CDK–cyclin complexes through the fission yeast cell cycle, we measured the protein kinase activity associated with cdc13, cig2 and cig1 in synchronous cultures of the *wee1-50* strain. Small cells in G_2 were isolated at 25°C by elutriation and then incubated at 36°C. Samples were collected every 20 min for two cell cycles, and histone H1 kinase activity was determined in immunoprecipitates of cig2 and cdc13; rum1 kinase activity was measured in immunoprecipitates

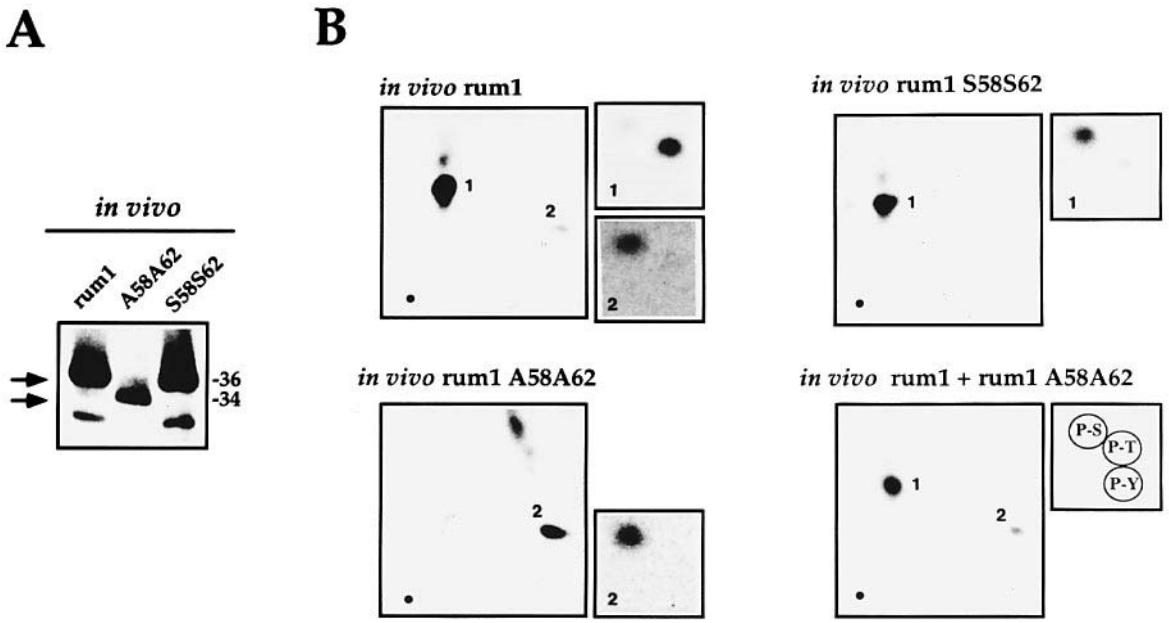

Fig. 8. p25^{rum1} is phosphorylated *in vivo* at residues T58 and T62. (**A**) Cultures of cells containing integrated copies of *rum1*$^+$, *rum1-A58A62* and *rum1-S58S62* in pREP81X were labelled with [^{32}P]phosphate (see Materials and methods). Extracts were prepared and immunoprecipitated with anti-rum1 antibodies. (**B**) Tryptic phosphopeptides of p25^{rum1}, p25$^{rum1\text{-}A58A62}$, p25$^{rum1\text{-}S58S62}$ and a mixture of the phosphopeptides of p25^{rum1} and p25$^{rum1\text{-}A58A62}$. Two main phosphopeptides were observed in ^{32}P-labelled p25^{rum1} (numbered 1 and 2). In p25^{rum1} and p25$^{rum1\text{-}A58A62}$, phosphopeptide 1 contained phosphothreonine while phosphopeptide 2 contained phosphoserine. In p25$^{rum1\text{-}S58S62}$, phosphopeptide 1 contained phosphoserine. Sample origins are indicated with a dot.

of cig1. As previously shown, cdc2–cig2 and cdc2–cdc13 H1 kinase activities oscillate through the cell cycle, with a peak of activity at the end of G_1 for cdc2–cig2 and in mitosis for cdc2–cdc13 (Figure 9; Martín-Castellanos *et al.*, 1996; Monderset *et al.*, 1996). cdc2–cig1-associated rum1 kinase activity was also periodic, increasing during S phase and rising to a peak in G_2 (Figure 9). This pattern of activity of the cdc2–cig1 complex mirrors exactly p25^{rum1} degradation; suggesting that if p25^{rum1} is an *in vivo* substrate for the cdc2–cig1 complex, it would be phosphorylated in S phase and G_2.

If phosphorylation of p25^{rum1} by cdc2–cig1 is important for targeting p25^{rum1} for degradation, then deletion of the *cig1*$^+$ gene should have an effect on the half-life of p25^{rum1}. To test this, we tried to perform pulse–chase experiments using [^{35}S]methionine. Unfortunately, we were unable to perform the chase under physiological conditions since the internal pool of methionine seems to be very large in *S.pombe*. We determined the half-life of p25^{rum1} after a short induction of the *rum1*$^+$ gene from the *nmt1* promoter in minimal media without thiamine and followed p25^{rum1} levels by Western blot after the addition of thiamine to repress the promoter (Figure 10). We found stabilization of p25^{rum1} when we deleted the *cig1*$^+$ gene. The half-life of p25^{rum1} in wild-type cells was ~40 min and it increased to >90 min in the *cig1*$^+$ deletion, suggesting that cdc2–cig1 has an active role in down-regulating p25^{rum1} levels *in vivo*.

Discussion

The *rum1*$^+$ gene encodes a CDK inhibitor important for regulating the G_1 phase of the fission yeast cell cycle (Moreno and Nurse, 1994; Moreno *et al.*, 1994; Correa-Bordes and Nurse, 1995; Labib *et al.*, 1995; Jallepalli and Kelly, 1996; Labib and Moreno, 1996; Martín-Castellanos *et al.*, 1996; Correa-Bordes *et al.*, 1997). p25^{rum1} has two functions in G_1: it determines the length of the pre-Start G_1 period and prevents mitosis from happening in early G_1 cells (Moreno and Nurse, 1994). Here we have presented evidence to explain these two effects of p25^{rum1}. We have shown that p25^{rum1} oscillates through the cell cycle and is present in the cell from anaphase until the end of G_1. In fission yeast, not all the cdc13 cyclin is degraded at the end of mitosis (Hayles and Nurse, 1995; Creanor and Mitchison, 1996; Yamano *et al.*, 1996; see also Figure 1B). This means that cells in early G_1 contain significant levels of cdc13 that could associate with cdc2 to form an active complex and which could trigger premature DNA replication or a lethal mitosis with unreplicated DNA. Thus, the presence of p25^{rum1} from anaphase until the end of G_1 could prevent cells from initiating S phase or mitosis either by inhibiting any residual cdc2–cdc13 activity or by increasing the turnover of cdc13 (Correa-Bordes *et al.*, 1997). p25^{rum1} has been shown to associate physically with cdc2–cdc13 in G_1, inhibiting its protein kinase activity (Correa-Bordes and Nurse, 1995).

Low CDK–cyclin activity before S phase is important for resetting the chromatin to a state which is permissive for DNA replication (Dahmann *et al.*, 1995; Nasmyth, 1996; Stern and Nurse, 1996; Wuarin and Nurse, 1996). It has been argued that dephosphorylation in G_1 of one or several proteins that bind to the origin recognition complex (ORC), such as MCMs or cdc18/Cdc6, is necessary for proper assembly of the DNA replication initiation complexes (Dahmann *et al.*, 1995; Nasmyth, 1996; Stern and Nurse, 1996; Wuarin and Nurse, 1996). In G_1, low CDK activity and high protein phosphatase activity provide conditions in which these dephosphorylation reactions can take place. In fission yeast, p25^{rum1} plays an active role

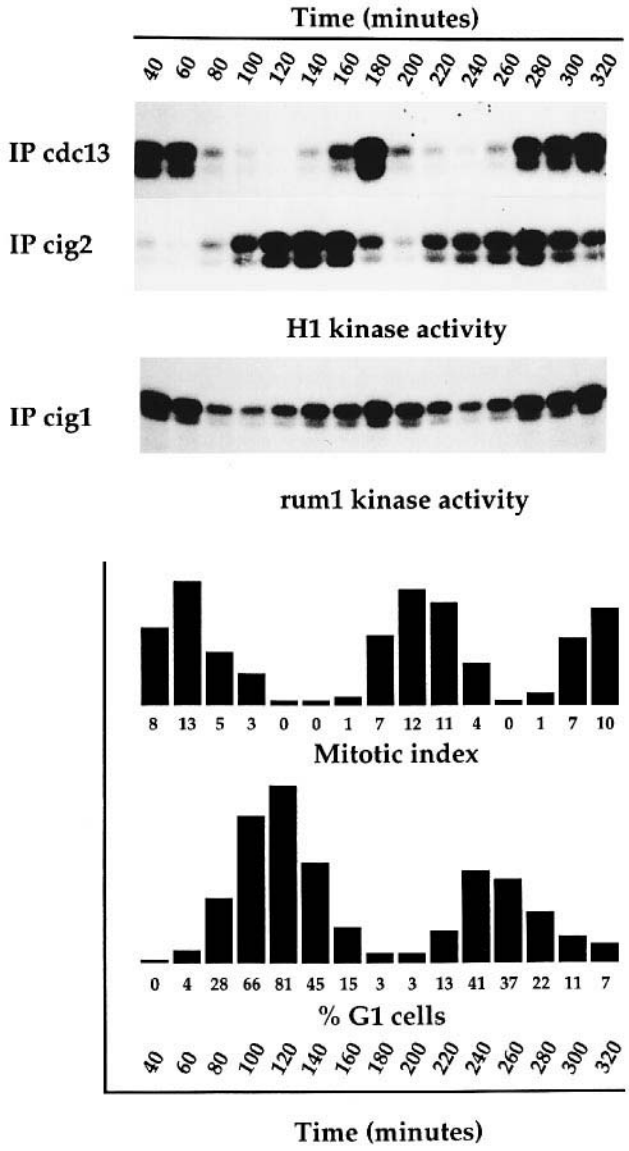

Fig. 9. Protein kinase activity of the different CDK–cyclin complexes through the fission yeast cell cycle. A synchronous population of *wee1-50* cells was prepared at 25°C by elutriation, the culture was incubated for 20 min at 25°C and then shifted up to 36°C. Samples were taken every 20 min to determine cdc13-, cig2- and cig1-associated kinase activity, the percentage of G_1 cells and the mitotic index. cdc13- and cig2-associated kinase activity was measured using histone H1 as substrate. cig1-associated kinase was determined using $p25^{rum1}$ as substrate. cdc13–cdc2 and cig1–cdc2 protein kinase activity peaks in mitosis while cig2–cdc2 peaks in G_1/S. The percentage of G_1 cells was measured by flow cytometry and the mitotic index by counting the number of cells in anaphase after DAPI staining (see Materials and methods).

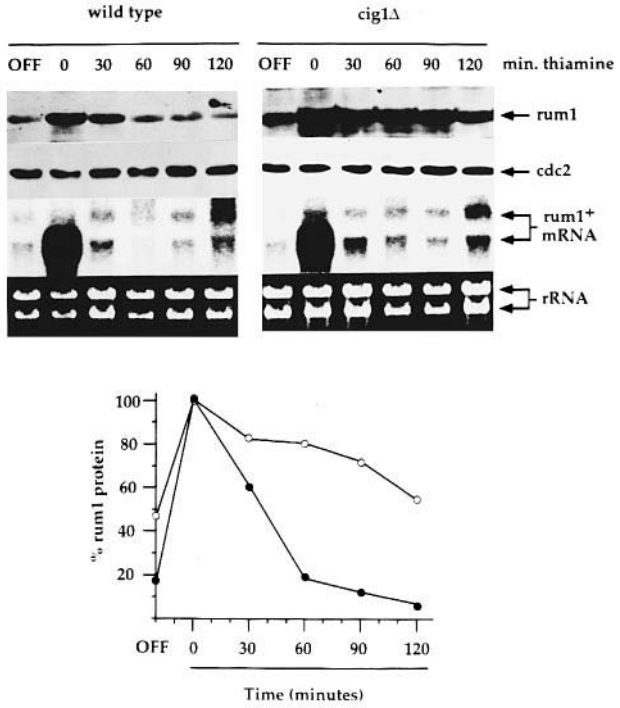

Fig. 10. $p25^{rum1}$ is stabilized in cells lacking the *cig1*$^+$ gene. The *rum1*$^+$ gene was overexpressed from the thiamine-repressible *nmt1* promoter (Maundrell, 1989), in wild-type (●) and *cig1*Δ (○) cells containing an integrated copy of pREP3X(*sup3-5*) *rum1*$^+$. Cells were grown to mid-exponential phase at 25°C in minimal medium containing 5 μg/ml thiamine, washed three times in minimal medium and resuspended in fresh medium lacking thiamine, at a density calculated to produce 4×10^6 cells/ml after 16 h, when expression from the *nmt1* promoter peaks. Thiamine was then added to the cultures to repress the *nmt1* promoter and samples for making RNA and protein were taken at the indicated times. $p25^{rum1}$ levels were determined by Western blot using affinity-purified R4 anti-$p25^{rum1}$ antibody and *rum1*$^+$ mRNA by Northern blot. Equal loading for immunoblots and Northern blots was confirmed by detection of $p34^{cdc2}$ and ethidium bromide staining of rRNA. Levels of $p25^{rum1}$ were quantified by densitometric analysis.

in this process by reducing the activity of cdc2–cyclinB complexes in G_1. Taking this into consideration, the cell cycle can be divided into two periods. The first period extends from anaphase until the end of G_1, and is characterized by high protein phosphatase activity and low cdc2–cyclin B activity. The second period starts at the end of G_1, when cdc2–cyclin B activity increases and the cells proceed to S phase and subsequently to mitosis. The alternation of these two periods allows dephosphorylation of cdc2–cyclinB substrates in G_1 before S phase, and their phosphorylation in S phase, G_2 and mitosis. These two periods could not co-exist. Protein phosphatases and CDK–cyclin complexes negatively regulate each other. Dephosphorylation of cdc2 on T167 by protein phosphatases leads to its inactivation (Gould *et al.*, 1991), and phosphorylation by CDK–cyclin complexes on T316 inactivates fission yeast and human protein phosphatase 1 (PP1) (Dohadwala *et al.*, 1994; Yamano *et al.*, 1994). In early G_1, when levels of the $p25^{rum1}$ CDK inhibitor are high, the effect of protein phosphatases predominates. As the cell grows during G_1, cig1, cig2 and cdc13 cyclins begin to accumulate and CDK activity eventually predominates at the end of G_1. These two biochemical states coincide in time with the pre-Start and post-Start periods, Start being the point where the switch occurs.

Phosphorylation of $p25^{rum1}$ by cdc2–cyclin complexes is important in regulating $p25^{rum1}$ stability. We have found that $p25^{rum1}$ is phosphorylated *in vivo* and that *rum1* mutants in two CDK phosphorylation sites, T58 and T62, show a gain-of-function phenotype. Cells bearing an integrated single copy of these mutant alleles expressed from the *rum1*$^+$ promoter showed a high frequency of diploidization and a long delay in G_1, especially in combination with the *cdc10-129* mutant at 25°C. These phenotypes are not the result of the mutant proteins

being more powerful inhibitors than the wild-type protein. Rather, they are more stable and do not oscillate through the cell cycle. The diploidization phenotype induced by these mutant alleles could be explained if stabilization of the mutant protein in G_2 occasionally reduces the level of the cdc2–cdc13 activity below the threshold level required to prevent initiation of another round of S phase within the same cell cycle (Hayles *et al.*, 1994). Thus, $p25^{rum1}$, which is normally present only in G_1, induces extra rounds of S phase when present in G_2.

Of the three cdc2–cyclin B complexes described in fission yeast, cdc2–cdc13 is the mitotic kinase while cdc2–cig2 is involved in the onset of S phase (Booher *et al.*, 1989; Moreno *et al.*, 1989; Fisher and Nurse, 1996; Martín-Castellanos *et al.*, 1996; Monderset *et al.*, 1996). The cdc2–cig1 complex might also contribute to the onset of S phase because a *cdc13*Δ *cig2*Δ double mutant can still undergo S phase while the *cdc13*Δ *cig2*Δ *cig1*Δ triple mutant cannot (Fisher and Nurse, 1996). $p25^{rum1}$ is an inhibitor of cdc2–cdc13 and cdc2–cig2 complexes but it does not inhibit cdc2–cig1 complexes (Figure 4B; Correa-Bordes and Nurse, 1995; Martín-Castellanos *et al.*, 1996). Here we present evidence suggesting that $p25^{rum1}$ may be a substrate for the cdc2–cig1 protein kinase. First, cdc2–cig1 is able to phosphorylate $p25^{rum1}$ efficiently and to induce a band shift similar to that observed *in vitro* with immunocomplexes of cdc2. The size of this band corresponds exactly to the size of $p25^{rum1}$ phosphorylated *in vivo*. In contrast, $p25^{rum1}$ is a poor substrate for cdc2–cdc13 and cdc2–cig2 complexes. Second, $p25^{rum1}$ is stabilized in cells lacking cig1, suggesting that $p25^{rum1}$ is a substrate for cig1-associated kinase and that this phosphorylation might be the signal that targets $p25^{rum1}$ for degradation. Deletion of $cig1^+$ specifically increases the half-life of $p25^{rum1}$, suggesting that cdc2–cig1 may be the principal trigger of $p25^{rum1}$ instability. This is consistent with the fact that cdc2–cig1 kinase activity accumulates during S phase and G_2, when $p25^{rum1}$ levels are low**.** We propose that one of the functions of cdc2–cig1 complexes is to relieve the effect of $p25^{rum1}$ inhibition over cdc2–cig2 and cdc2–cdc13 complexes, ensuring that $p25^{rum1}$ is destroyed by the time cells undergo DNA replication and is absent in S phase and G_2. However, in addition to cdc2–cig1, there must be other cdc2–cyclin complexes able to phosphorylate $p25^{rum1}$ because in cells lacking cig1, $p25^{rum1}$ is still unstable and these cells do not show the phenotypes that we observed in the *rum1-A58A62* mutant. We currently are addressing this point by constructing multiple deletions of fission yeast cyclins.

We have also shown that $p25^{rum1}$ is stabilized in the *mts3-1* mutant defective in subunit 14 of the 26S proteasome (Gordon *et al.*, 1996), suggesting that degradation of $p25^{rum1}$ occurs through the proteasome-dependent proteolytic pathway. Further support for this idea comes from the recent finding that $p25^{rum1}$ is stabilized in the fission yeast *pop1-1* mutant, defective in a protein homologue of the budding yeast Cdc4 (Kominami and Toda, 1997). As in *S.cerevisiae*, the fission yeast Cdc4 homologue could be part of a complex involved in the ubiquitination and degradation of multiple targets at the end of G_1, including G_1 cyclins and the CDK inhibitor $p25^{rum1}$. Proteolysis of other CDK inhibitors such as $p40^{SIC1}$ and $p27^{KIP1}$ is mediated by the ubiquitin-dependent proteolytic pathway (Schwob *et al.*, 1994; Pagano *et al.*, 1995; Verma *et al.*, 1997). Interestingly, *pop1* mutant cells like *rum1-A58A62* cells diploidized at high frequency (Kominami and Toda, 1997). Degradation of inhibitors is a recurrent theme in biology (Murray, 1995). In the immune system, the IκB-α family of inhibitors prevents nuclear localization of the transcriptional activator NF-κB (Thanos and Maniatis, 1995). Extracellular signals including tumour necrosis factor-α (TNF-α), lipopolysaccharide (LPS) and interleukin-1 (IL-1) induce rapid degradation of IκB-α (Pahl and Bauerle, 1996). Degradation of IκB-α is preceded by phosphorylation on two serine residues, S32 and S36, that convert this protein into an efficient substrate for the protein ubiquitination machinery (Brown *et al.*, 1995; Chen *et al.*, 1995; Traenckner *et al.*, 1995). In this regard, it is interesting that the two putative phosphorylation sites in $p25^{rum1}$ are located in the amino-terminus region and are also separated by four amino acids.

Is $p25^{rum1}$ function likely to be conserved in other eukaryotes? $p25^{rum1}$ is a CDK inhibitor that has specificity for S phase and mitotic cdc2–cyclin kinases. This is similar to the situation in budding yeast, where $p40^{SIC1}$ has been shown to inhibit specifically Cdc28–Clb-associated kinases, preventing the initiation of S phase and mitosis during G_1 (Schwob *et al.*, 1994; Nasmyth, 1996). Like $p25^{rum1}$, $p40^{SIC1}$ is stabilized during anaphase and is degraded at the end of G_1 through the Cdc4–Cdc34–Cdc53 ubiquitin-dependent proteolytic pathway (Donovan *et al.*, 1994; Schwob *et al.*, 1994). Degradation of $p40^{SIC1}$ is also thought to depend on Cdc28 phosphorylation by the Cdc28–Cln kinases (Schwob *et al.*, 1994; Schneider *et al.*, 1996). In addition, there is sequence similarity in the CDK inhibitory domain between $p40^{SIC1}$ and $p25^{rum1}$, and expression of *SIC1* rescues a deletion of $rum1^+$ in fission yeast (A.Sánchez, I.González, M.Arellano and S.Moreno, submitted). Overproduction of *SIC1* in fission yeast also induces re-replication (Jallepalli and Kelly, 1996; our unpublished results), suggesting that $p40^{SIC1}$ and $p25^{rum1}$ inhibit a similar set of CDK–cyclin complexes in fission yeast. None of the CDK inhibitors described so far in animal cells has a specificity for the Cdc2–cyclin B kinase (Sherr and Roberts, 1995; Elledge *et al.*, 1996), leaving open the question of whether animal cells have found an alternative mechanism to restrain the mitotic kinase between anaphase and passage through the restriction point.

Materials and methods

Fission yeast strains and methods

Strains used in this study are congenic with the *972 h*$^-$ strain of *S.pombe* and are listed in Table I. Growth conditions and strain manipulations were as described by Moreno *et al.* (1991). The *cig1*Δ*::ura4*$^+$ *ura4-D18 h*$^-$ strain was described by Bueno *et al.* (1991), and involves deletion of the entire open reading frame (ORF). The *cig2*Δ*::ura4*$^+$ *ura4-D18 h*$^-$ strain was described by Obara-Ishihara and Okayama (1994), and involves deletion of the N-terminal 80% of the protein. The *rum1*Δ*::ura4*$^+$ *ura4-D18 leu1-32 ade6-M216 h*$^-$ strain was described by Moreno and Nurse (1994), and involves deletion of the entire ORF. Since deletion of $rum1^+$causes sterility, all the crosses involving a deletion of $rum1^+$ were done by transforming with pREP3X-$rum1^+$, so that $rum1^+$is expressed from a plasmid, and the double mutants were checked subsequently to ensure that the plasmid had been lost. Tetrad analysis was performed to construct double mutants, and the identity of

Table I. *Schizosaccharomyces pombe* strains

Strain	Genotype	Source
P1	*972 h*$^{-}$	P.Nurse
P43	*leu1-32 h*$^{-}$	P.Nurse
S391	*wee1-50 cig2-HA h*$^{-}$	S.Moreno
S445	*mts3-1 leu1-32 h*$^{-}$	C.Gordon
S432	*cig1Δ::ura4*$^{+}$ *ura4-D18 h*$^{-}$	A.Bueno
S349	*cig2Δ::ura4*$^{+}$ *ura4-D18 h*$^{-}$	H.Okayama
S487	*rum1Δ::ura4*$^{+}$ *ura4-D18 leu1.32 h*$^{+}$	S.Moreno
S478	*intpREP81Xrum1::sup3.5[LEU2] ade6-704 leu1-32 ura4-D18 h*$^{+}$	this study
S401	*intpREP81Xrum1-T58A::sup3.5[LEU2] ade6-704 leu1-32 ura4-D18 h*$^{+}$	this study
S402	*intpREP81Xrum1-T62A::sup3.5[LEU2] ade6-704 leu1-32 ura4-D18 h*$^{+}$	this study
S479	*intpREP81Xrum1-T58/62A::sup3.5[LEU2] ade6-704 leu1-32 ura4-D18 h*$^{+}$	this study
S552	*rum1Δ::ura4*$^{+}$ *ura4-D18 leu1.32 intpREP81Xrum1 h*$^{+}$	this study
S553	*rum1Δ::ura4*$^{+}$ *ura4-D18 leu1.32 intpREP81Xrum1-T58/62A h*$^{+}$	this study
S549	*rum1Δ::ura4*$^{+}$ *ura4-D18 leu1.32 intpREP81Xrum1-T58/62S h*$^{+}$	this study
S366	*rum1Δ::ura4*$^{+}$ *intpIRT2rum1::LEU2 ura4-D18 leu1-32 h*^{90}	this study
S484	*rum1Δ::ura4*$^{+}$ *intpIRT2rum1-T58A::LEU2 ura4-D18 leu1-32 h*^{90}	this study
S485	*rum1Δ::ura4*$^{+}$ *intpIRT2rum1-T62A::LEU2 ura4-D18 leu1-32 h*^{90}	this study
S486	*rum1Δ::ura4*$^{+}$ *intpIRT2rum1-T58/62A::LEU2 ura4-D18 leu1-32 h*^{90}	this study
S348	*cdc10.129 rum1Δ::ura4*$^{+}$ *intpIRT2rum1::LEU2 leu1.32 ura4-D18 h*^{90}	this study
S482	*cdc10.129 rum1Δ::ura4*$^{+}$ *intpIRT2rum1-T58/62A::LEU2 leu1-32 ura4-D18 h*^{90}	this study
S63	*intpREP6Xrum1::sup3.5 ade6.704 leu1-32 ura4-D18 h*$^{+}$	this study
S428	*intpREP6Xrum1::sup3.5 cig1Δ::ura4 ade6-704 leu1-32 ura4-D18 h*$^{-}$	this study

these mutants was confirmed by Southern blotting. Yeast transformation was carried out using the lithium acetate transformation protocol (Moreno *et al.*, 1991).

All experiments in liquid culture were carried out in minimal medium (EMM) containing the required supplements, starting with a cell density of 2–4×10^6 cells/ml, corresponding to mid-exponential phase growth. Temperature shift experiments were carried out using a water bath at 36°C.

To induce expression from the *nmt1* promoter, cells were grown to mid-exponential phase in EMM containing 5 μg/ml thiamine, then spun down and washed four times with minimal medium, before resuspending in minimal medium lacking thiamine at a density calculated to produce 4×10^6 cells/ml at the time of peak expression from the *nmt1* promoter.

Plasmids

Plasmids are listed in Table II. A 3.8 kb *Pst*I–*Bam*HI fragment containing the *rum1*$^{+}$ gene was cloned into pTZ18R. This plasmid was used to obtain the different *rum1* mutants by site-directed mutagenesis using the Muta-gene phagemid *in vitro* mutagenesis kit (Bio-Rad) and the following oligonucleotides: T5A, 5′-CATAGGTGGTGCTGAAGGTTCC-3′; T13A T16A S19A, 5′-CCCAGGAGCCTCTGGGGCAGATGGAGCACACAA-3′; T58A, 5′-GTTTTAGCAGGTGCAGGTGGAAATGT-3′; T62A, 5′-GCTTTTTGGGAGCTTTAGCAGGTGT-3′; T110A, 5′-GGAGGAGGAGCAGGCTTTCTC-3′; S212A, 5′-GATTTTTGTGGTGCTGAATACGC-3′; T58A T62A, 5′-GCTTTTTGGGAGCTTTAGCAGGTGCAGGTGGAAATGTG-3′; T58S T62S, 5′-GCTTTTTGGGAGATTTAGCAGGTGAAGGTGGAAATGTG-3′.

The underlined nucleotides contain the mutated sequence. All the mutants were sequenced after the mutagenesis. The 3.8 kb *Pst*I–*Bam*HI fragments were then subcloned into the pIRT2 vector. To make the constructions in pREP-3X and the pREP-81X, DNA from the different mutants was amplified by PCR using the high-fidelity Pwo polymerase (Boehringer Manheim) and the following oligos, 18mer 5′ oligonucleotide 5′-CCGCTCGAGACAAAA-3′, where the underlined sequence contains an *Xho*I site, and a 28mer 3′ oligonucleotide with the sequence 5′-GGGCATTTATATAAACGGGATCCAACAC-3′, where the underlined sequence contains a *Bam*HI site. The 700 bp PCR products were digested with *Xho*I and *Bam*HI and subcloned into pREP-3X and pREP-81X. The pREP1-His$_6$-ubiquitin plasmid was a gift of Dr Hiroyuki Yamano.

Synchronous cultures

wee1-50 h^{-} cells were grown at 25°C in EMM. Cells were synchronized at 25°C using a JE-5.0 elutriation system (Beckman Instruments, Inc.) and then shifted to 36°C, resulting in entry into mitosis at a reduced cell size. Samples were taken every 20 min during two cell cycles for making RNA or protein extracts and for flow cytometry analysis.

Table II. Plasmid list

pREP3X
pREP81X
pREP (*sup 3-5*) 3X-*rum1*$^{+}$
pREP (*sup 3-5*) 81X-*rum1*$^{+}$
pREP (*sup 3-5*) 81X-*rum1*-A5
pREP (*sup 3-5*) 81X-*rum1*-A13A16A19
pREP (*sup 3-5*) 81X-*rum1*-A58
pREP (*sup 3-5*) 81X-*rum1*-A62
pREP (*sup 3-5*) 81X-*rum1*-A58A62
pREP (*sup 3-5*) 81X-*rum1*-A110
pREP (*sup 3-5*) 81X-*rum1*-A212
pREP (*sup 3-5*) 81X-*rum1*-S58S62
pREP1-His$_6$-ubiquitin
pIRT2
pIRT2-*rum1*$^{+}$
pIRT2-*rum1*-A5
pIRT2-*rum1*-A13A16A19
pIRT2-*rum1*-A5A13A16A19
pIRT2-*rum1*-A58
pIRT2-*rum1*-A62
pIRT2-*rum1*-A58A62
pIRT2-*rum1*-A110
pIRT2-*rum1*-A212

RNA preparation and Northern blots

RNA from elutriated cells was prepared by glass beads lysis in the presence of phenol. RNA gels were run in the presence of formaldehyde, transferred to GeneScreen Plus (NEN, Dupont) and probed according to the manufacturer's instructions. Quantification of ^{32}P signals was performed using a Fuji PhosphorImager.

Protein extracts and Western blots

Total protein extracts were prepared from 3×10^8 cells collected by centrifugation, washed in Stop buffer (150 mM NaCl, 50 mM NaF, 10 mM EDTA, 1 mM NaN_3 pH 8.0), and resuspended in 25 μl of RIPA buffer (10 mM sodium phosphate, 1% Triton X-100, 0.1% SDS, 10 mM EDTA, 150 mM NaCl, pH 7.0) containing the following protease inhibitors, 10 μg/ml leupeptin, 10 μg/ml aprotinin, 10 μg/ml pepstatin, 10 μg/ml soybean trypsin inhibitor, 100 μM 1-chloro-3-tosylamido-7-amino-L-2-heptanone (TLCK), 100 μM *N*-tosyl-L-phenylalanine chloromethyl ketone (TPCK), 100 μM phenylmethylsulfonyl fluoride (PMSF),

1 mM phenanthroline and 100 μM *N*-acetyl-leu-leu-norleucinal. Cells were boiled for 5 min, broken using 750 mg of glass beads (0.4 mm Sigma) for 15 s in a Fast-Prep machine (Bio101 Inc.), and the crude extract was recovered by washing with 0.5 ml of RIPA.

For Western blots, 100 μg of total protein extract was run on a 14% SDS–polyacrylamide gel, transferred to nitrocellulose and probed with affinity-purified SP4 anti-cdc13 (1:250), PN24 anti-cdc2 (1:250) or R3 (or R4) anti-rum1 polyclonal antibodies. Goat anti-rabbit antibody conjugated to horseradish peroxidase (1:3500) was used as secondary antibody. Immunoblots were developed using the ECL kit (Amersham). Quantification of ECL signals was performed by densitometric analysis.

Detection of $p25^{rum1}$–His_6-ubiquitin conjugates

To purify the His_6-ubiquitin $p25^{rum1}$ conjugates, we made extracts from 3×10^8 cells essentially as described previously by Treier *et al.* (1994) and Musti *et al.* (1996). Briefly, cells were lysed in 8 M urea, 100 mM sodium phosphate pH 8.0, 5 mM imidazole. Cell extracts were centrifugated at 4°C in a microfuge for 5 min, and the protein concentration determined by BCA protein assay reagent (Pierce). Six mg of extract were mixed with Ni^{2+}-NTA agarose (Quiagen) and incubated for 4 h at room temperature in a roller. The Ni^{2+}-NTA resin was washed successively with: 8 M urea, 0.1 M sodium phosphate pH 8.0; 8 M urea, 0.1 M sodium phosphate pH 5.8; 8 M urea, 0.1 M sodium phosphate pH 8.0; 8 M urea, 0.1 M sodium phosphate pH 8.0; protein buffer (1:1); 8 M urea, 0.1 M sodium phosphate pH 8.0; protein buffer (1:3); protein buffer; protein buffer, 10 mM imidazole; followed by elution in protein buffer plus 200 mM imidazole. The protein buffer contains 50 mM sodium phosphate pH 8.0, 100 mM KCl, 20% glycerol and 0.2% NP-40. The eluate was diluted in 2× sample buffer, boiled for 5 min and analysed by Western blot with R4 affinity-purified anti-rum1 antibody (1:50).

Protein extracts and kinase assays

For kinase assays, extracts from 3×10^8 cells were made using HB buffer (Moreno *et al.*, 1989, 1991). Cell extracts were spun at 4°C in a microfuge for 5 min, and the protein concentration determined by the BCA protein assay reagent (Pierce). Samples of 0.5 mg (in *wee1.50 h*$^-$ synchronous culture) and 1.5 mg (in *in vitro* phosphorylation assays) were immunoprecipitated at 0°C for 1 h, using 2 μl of SP4 anti-cdc13, 2 μl of anti-cig2, 2 μl of 9830-U anti-cig1 or 2 μl of C2 anti-cdc2 polyclonal antibodies. Thirty μl of protein A–Sepharose was then added for 30 min at 4°C and the immunoprecipitates washed three times with 1 ml of HB buffer. Immunoprecipitates (~20 μl) were resuspended in 20 μl of HB containing 50 μM ATP, 0.5 mg/ml substrate histone H1 (Calbiochem) (or 0.5 mg/ml of $p25^{rum1}$ or $p25^{rum\text{-}A58A62}$) and 40 μCi/ml [γ-^{32}P]ATP, and incubated at 25°C for 30 min. The reactions were stopped with 40 μl of 2× SDS–PAGE sample buffer, denatured at 100°C for 5 min and samples were run on a 14% SDS–polyacrylamide gel. Phosphorylated proteins were detected by autoradiography.

Phospholabelling of $p25^{rum1}$

We used the procedures described by Gould and Nurse (1989) and Den Haese *et al.* (1995) with minor modifications. Cells were grown for 12 h in phosphate-free minimal medium containing 50 μM NaH_2PO_4 and appropriate supplements to a density of 5×10^6 cells/ml. Five ml cultures were spun down, resuspended in 5 ml of fresh medium and 1.2 mCi of [^{32}P]orthophosphate was added. To label cells that were overexpressing $p25^{rum1}$, $p25^{rum1\text{-}A58A62}$ or $p25^{rum1\text{-}S58S62}$ proteins, cells of the strains S552, S553 and S549 containing integrated copies of *rum1*$^+$, *rum1-A58A62* and *rum1-S58S62* in pREP81X were grown to mid-log phase in the presence of 5 μg/ml thiamine, washed five times in phosphate free-minimal medium lacking thiamine, and inoculated into fresh medium. After 18 h of growth at 32°C in the absence of thiamine, the cells were pelleted by centrifugation and resuspended in 20 ml of phosphate-free minimal medium containing 50 μM NaH_2PO4 and 5 mCi of [^{32}P]orthophosphate at a concentration of 6×10^6 cells/ml in the absence of thiamine. In all the experiments, the cells were labelled for 4 h at 32°C.

Cell lysates were prepared as described above and were immediately made to 1% SDS, 1 mM dithiothreitol and boiled for 3 min. The extracts were then diluted 10-fold in RIPA buffer lacking SDS, and centrifugated for 15 min at 4°C at 10 000 *g*. Immunoprecipitation was performed for 1 h on ice using 4 μl of anti-rum 1 (R4) serum followed by incubation with protein A–Sepharose (Gould and Nurse, 1989; Den Haese *et al.*, 1995). Immunoprecipitates were boiled for 3 min in SDS–PAGE sample buffer, resolved on 14% SDS–polyacrylamide gels and transferred to Immobilon-P membrane (Millipore). Bands were visualized after autoradiography using Kodak Biomax films at –70°C with intensifying screens.

Phosphopeptide mapping and phosphoamino acid analysis

Phosphopeptide maps were accomplished as described previously by Boyle *et al.* (1991) and Van der Geer and Hunter (1994). ^{32}P-Labelled bands were cuts from the Immobilon-P membrane and trypsinized in 200 μl of 50 mM sodium bicarbonate pH 7.3 containing 15 μg of trypsin-TPCK (Worthington Biochemical Corp.). After 12 h at 37°C, 15 μg of trypsin was added and digested for another 4 h at 37°C. Phosphopeptides were separated on TLC plates by electrophoresis at pH 1.9 (formic acid:acetic acid:water; 50:156:1794) for 60 min at 1 kV, followed by ascending chromatography in *n*-butanol:pyridine:acetic acid:water (75:50:15:60). Individual phosphopetides were recovered as described by Van deer Geer and Hunter (1994), eluted in buffer at pH 1.9 and evaporated.

To determine the phosphoamino acid composition, the phosphopeptide was dissolved in 6 M HCl and incubated for 60 min at 110°C. The hydrolysis products were separated by electrophoresis in two dimensions on TLC plates at pH 1.9 and 3.5 as described by Boyle *et al.* (1991). Peptides and phosphoamino acids were visualized by autoradiography on Kodak Biomax film at –70°C with intensifying screens.

Purification of $p25^{rum1}$ from *E.coli*

A 0.7 kb *Nde*I–*Bam*HI DNA fragment containing the *rum1*$^+$ or *rum1-A58A62* ORF was cloned into pRK171 vector and transformed into the *E.coli* strain BDL21(DE3). Three hundred ml of a culture in LB containing 50 μg/ml ampicillin was grown at 37°C until OD_{600} = 0.7 and induced with 0.4 mM isopropyl-β-D-thiogalactopyranoside (IPTG) for 4 h. The cells were harvested by centrifugation, resuspended in 25 ml of ice-cold lysis buffer (25 mM Tris–HCl pH 7.5, 50 mM NaCl, 1 mM EDTA, 0.1 mM PMSF, 0.3% Triton X-100) and sonicated on ice 10 times for 10 s at medium power. The lysate was centrifugated for 20 min at 10 000 r.p.m. at 4°C and the supernatant containing $p25^{rum1}$ soluble protein was loaded twice onto an anion exchanger Q-Sepharose (Sigma) column equilibrated with buffer A (50 mM Tris–HCl pH 7.5, 50 mM NaCl). The column was washed with buffer A. The flow-through and the wash were mixed and loaded into a cation exchanger S-Sepharose (Pharmacia) column equilibrated with buffer A. The protein was eluted from the column with a 50–500 mM NaCl salt gradient in 50 mM Tris–HCl pH 7.5. The fractions containing $p25^{rum1}$ were pooled and dialysed twice against distilled water. Protein concentration was determined by BCA protein assay reagent (Pierce), and 100 μg aliquots were lyophilized and stored at –20°C.

$p25^{rum1}$ inhibition assays

Purified $p25^{rum1}$ or $p25^{rum1\text{-}A58A62}$ was added to the immunoprecipitates before the addition of the kinase assay buffer. The histone H1 kinase reactions were carried out in the same conditions as described above.

Flow cytometry and microscopy

About 10^7 cells were spun down, washed once with water, fixed in 70% ethanol and processed for flow cytometry or 4′,6'-diamidino-2-phenylindole (DAPI) staining, as described previously (Sazer and Sherwood, 1990; Moreno *et al.*, 1991). A Becton-Dickinson FACScan was used for flow cytometry. To estimate the proportion of G_1 cells, we determined the percentage of cells with a DNA content less than a value mid-way between 1C and 2C. The mitotic index was determined by counting the percentage of anaphase cells (cells with two nuclei and without septum) after DAPI staining.

Acknowledgements

We would like to thank Pilar Bolaños for the Northern blots shown in Figures 1C and 10, Jorge Martín-Pérez for help with the phosphopeptide maps and phosphoamino acid analysis, Jaime Correa-Bordes, Avelino Bueno, Paul Russell, Hiroyuki Yamano and Colin Gordon for the gift of plasmids, antibodies and strains, Jaime Correa-Bordes, Paul Nurse, Kin-ichiro Kominami and Takashi Toda for sharing their unpublished data, and Chris Norbury and Karim Labib for valuable comments to the manuscript. We gratefully acknowledge financial support provided to our laboratory by the CICYT, the Human Frontier Science Program and the Ramón Areces Foundation.

References

Adachi,Y. and Laemmli,U.K. (1994) Study of the cell cycle-dependent assembly of the DNA pre-replication centres in *Xenopus* egg extracts. *EMBO J.*, **13**, 4153–4164.

Amon,A., Irniger,S. and Nasmyth,K. (1994) Closing the cell cycle circle in yeast: G_2 cyclin proteolysis initiated at mitosis persits until the activation of G_1 cyclins in the next cycle. *Cell*, **77**, 1037–1050.

Bai,C., Sen,P., Hofmann,K., Ma,L., Goebl,M., Harper,J.W. and Elledge, S.J. (1996) *SKP1* connects cell cycle regulators to the ubiquitin proteolysis machinery through a novel motif, the F-Box. *Cell*, **86**, 263–274.

Boyle,W.J, Van der Geer,P. and Hunter,T. (1991) Phosphopeptide mapping and phosphoamino acid analysis by two-dimensional separation on thin-layer cellulose plates. *Methods Enzymol.*, **201**, 110–149.

Booher,R.N., Alfa,C.E., Hyams,J.S. and Beach,D. (1989) The fission yeast cdc2/cdc13/suc1 protein kinase: regulation of catalytic activity and nuclear localization. *Cell*, **58**, 485–497.

Brandeis,M. and Hunt,T. (1996) The proteolysis of mitotic cyclins in mammalian cells persist from the end of mitosis until the onset of S-phase. *EMBO J.*, **15**, 5280–5289.

Broek,D.,Bartlett,R., Crawford,K. and Nurse, P. (1991) Involvement of $p34^{cdc2}$ in establishing the dependency of S phase on mitosis. *Nature*, **349**, 388–393.

Brown,K., Gerstberger,S., Carlson,L., Franzoso,G. and Sienblist,U. (1995) Control of IκB-α proteolysis by site specific, signal induced phosphorylation. *Science*, **267**, 1485–1488.

Bueno,A., Richardson,H., Reed,S.I. and Russell,P. (1991) A fission yeast B-type cyclin functioning early in the cell cycle. *Cell*, **66**, 149–160.

Chang,F. and Herskowitz,I. (1990) Identification of a gene necessary for the cell cycle arrest by a negative growth factor of yeast: FAR1 is an inhibitor of a G_1 cyclin, CLN2. *Cell*, **63**, 999–1011.

Chen,Z., Hagler,J., Pallombella,V.J., Malandri,F., Scherer,D., Ballard,D. and Maniatis,T. (1995) Signal-induced site-specific phosphorylation targets IκB-α to the ubiquitin–proteasome pathway. *Genes Dev.*, **9**, 1586–1597.

Clurman,B.E., Sheaff,R.J.,Thress,K., Groudine,M. and Roberts,J.M. (1996) Turnover of cyclinE by the ubiquitin–proteasome pathway is regulated by CDK2 binding and cyclin phosphorylation. *Genes Dev.*, **10**, 1979–1990.

Connelly,C. and Hieter,P. (1996) Budding yeast *SKP1* encodes an evolutionary conserved kinetochore protein required for cell cycle progression. *Cell*, **86**, 275–285.

Correa-Bordes,J. and Nurse,P. (1995) $p25^{rum1}$ orders S-phase and mitosis by acting as an inhibitor of the $p34^{cdc2}$ mitotic kinase. *Cell*, **83**, 1001–1009.

Correa-Bordes,J., Gulli,M.P. and Nurse,P. (1997) $p25^{rum1}$ promotes proteolysis of the mitotic B-cyclin $p56^{cdc13}$ during G_1 of the fission yeast cell cycle. *EMBO J.*, **16**, 4657–4664.

Creanor,J. and Mitchison,J.M. (1996) The kinetics of the B cyclin $p56^{cdc13}$ and the phosphatase $p80^{cdc25}$ during the cell cycle of the fission yeast *Schizosaccharomyces pombe*. *J. Cell Sci.*, **109**, 1647–1653.

Dahmann,C., Diffley,J.F.X. and Nasmyth,K. (1995) S-phase-promoting cyclin-dependent kinases prevent re-replication by inhibiting the transition of replication origins to a pre-replicative state. *Curr. Biol.*, **5**, 1257–1269.

Den Haese,G.J., Walworth,N., Carr,A.M. and Gould,K. (1995) The wee1 protein kinase regulates T14 phosphorylation of fission yeast cdc2. *Mol. Biol. Cell.*, **6**, 371–385.

Deshaies,R.J. (1995) The self-destructive personality of a cell cycle in transition. *Curr. Opin. Cell Biol.*, **7**, 781–789.

Deshaies,R.J., Chau,V. and Kirschner,M.W. (1995) Ubiquitination of the G_1 cyclin Cln2 by a Cdc34-dependent pathway. *EMBO J.*, **14**, 303–312.

Diehl,J.A., Zindy,F. and Sherr,C.J. (1997) Inhibition of cyclin D1 phosphorylation on threonine-286 prevents its rapid degradation via the ubiquitin–proteasome pathway. *Genes Dev.*, **11**, 957–972.

Dirick,L., Bohm,T. and Nasmyth,K. (1995) Roles and regulation of Cln–Cdc28 kinases at the start of the cell cycle of *Saccharomyces cerevisiae*. *EMBO J.*, **14**, 4803–4813.

Dohadwala,M., Cruz e Silva,E.F., Hall,F.L., Williams,R.T., Carbonaro-Hall,D.A., Nairn,A.C., Greegard,P. and Berndt,N. (1994) Phosphorylation and inactivation of protein phosphatase 1 by cyclin-dependent kinases. *Proc. Natl Acad. Sci. USA*, **91**, 6408–6412.

Donovan,J.D., Toyn,J.H.,Johnson,A.L. and Johnson,L. (1994) $p40^{SDB25}$, a putative CDK inhibitor, has a role in the M/G_1 transition in *Saccharomyces cerevisiae*. *Genes Dev.*, **8**, 1640–1653.

Elledge,S.J., Winston,J. and Harper,J.W. (1996) A question of balance: the role of cyclin-kinase inhibitors in development and tumorigenesis. *Trends Cell Biol.*, **6**, 388–392.

Fisher,D. and Nurse,P. (1995) Cyclins of the fission yeast *Schizosaccharomyces pombe*. *Semin. Cell Biol.*, **6**, 73–78.

Fisher,D. and Nurse,P. (1996) A single fission yeast mitotic cyclin B $p34^{cdc2}$ kinase promotes both S-phase and mitosis in the absence of G_1 cyclins. *EMBO J.*, **15**, 850- 860

Forsburg,S.L. and Nurse,P. (1991) Identification of a G_1-type cyclin puc1 in the fission yeast *Schizosaccharomyces pombe*. *Nature*, **351**, 245–248.

Forsburg,S.L. and Nurse,P. (1994) Analysis of *Schizosaccharomyces pombe* cyclin puc1: evidence for a role in cell cycle exit. *J. Cell Sci.*, **107**, 601–613.

Funabiki,H., Yamano,H., Kumada,K., Nagao,K., Hunt,T. and Yanagida,M. (1996) Cut2 proteolysis required for sister-chromatid separation in fission yeast. *Nature*, **381**, 438–441.

Glotzer,M., Murray,A.W. and Kirschner,M.W. (1991) Cyclin is degraded by the ubiquitin pathway. *Nature*, **349**, 132–138.

Goebl,M.G., Yochem,J., Jentsch,S., McGrath,J.P., Varshavsky,A. and Byers,B. (1988) The yeast cell cycle gene *CDC34* encodes a ubiquitin-conjugating enzyme. *Science*, **241**, 1331–1335.

Gordon,C., McGurk,G., Wallace,M. and Hastie,N.D. (1996) A conditional lethal mutant in the fission yeast 26S protease subunit mts3 is defective in metaphase to anaphase transition. *J. Biol. Chem.*, **271**, 5704–5711.

Gould,K.L and Nurse,P. (1989) Tyrosine phosphorylation of the fission yeast cdc2 protein kinase regulates entry into mitosis. *Nature*, **342**, 39–45.

Gould,K., Moreno,S., Owen,D., Sazer,S. and Nurse,P. (1991) Phosphorylation at T^{167} is required for *Schizosaccharomyces pombe* $p34^{cdc2}$ function. *EMBO J.*, **10**, 3297–3309.

Hartwell,L.H., Culotti,J., Pringle,J. and Reid,B.J. (1974) Genetic control of the cell division cycle in yeast. *Science*, **183**, 46–51.

Hayles,J. and Nurse,P. (1995) A pre-Start checkpoint preventing mitosis in fission yeast acts independently of $p34^{cdc2}$ tyrosine phosphorylation. *EMBO J.*, **14**, 2760–2771.

Hayles,J., Fisher,D., Woollard,A. and Nurse,P. (1994) Temporal order of S phase and mitosis in fission yeast is determined by the state of the $p34^{cdc2}$–mitotic B cyclin complex. *Cell*, **78**, 813–822.

Hershko,A., Ganoth,D., Pehrson,J., Palazzo,R.E. and Cohen,L.H. (1991) Methylated ubiquitin inhibits cyclin degradation in clam embryo extracts. *J. Biol. Chem.*, **266**, 16376–16379.

Hershko,A., Ganoth,D., Sudakin,V., Dhan,A., Cohen,L.H., Luca,F.C., Ruderman,J.V. and Eytan,E. (1994) Components of a system that ligates cyclin to ubiquitin and their regulation by the protein kinase cdc2. *J. Biol. Chem.*, **266**, 16376–16370.

Hirano,T., Hiraoka,Y. and Yanagida,M. (1988) A temperature-sensitive mutation of the *Schizosaccharomyces pombe* gene $nuc2^+$ that encodes a nuclear scaffold-like protein blocks spindle elongation in mitotic anaphase. *J.Cell Biol.*, **106**, 1171–1183.

Irniger,S., Piatti,S., Michaelis,C. and Nasmyth,K. (1995) Genes involved in sister chromatid separation are needed for B-type cyclin proteolysis in budding yeast. *Cell*, **81**, 269–277.

Jallepalli,P.V. and Kelly,T.J. (1996) rum1 and cdc18 link inhibition of cyclin-dependent kinase to the initiation of DNA replication in *Schizosaccharomyces pombe*. *Genes Dev.*, **10**, 541–552.

Kelly,T.J., Martin, G.S., Forsburg,S.L., Stephen,R.J., Russo,A. and Nurse,P. (1993) The fission yeast $cdc18^+$ gene product couples S-phase to Start and mitosis. *Cell*, **74**, 371–382.

King,R.W., Peters,J.M., Tugendreich,S., Rolfe,M., Hieter,P. and Kirschner,M.W. (1995) A 20S complex containing CDC27 and CDC16 catalyzes the mitosis-specific conjugation of ubiquitin to cyclin B. *Cell*, **81**, 279–288.

Kipreos,E.T., Lander,L.E., Wing,J.P., He,W.W. and Hedgecock,E.M. (1996) *cul-1* is required for cell cycle exit in *C.elegans* and identifies a novel gene family. *Cell*, **85**, 829–839.

Kominami,K. and Toda,T. (1997) Fission yeast WD-repeat protein pop1 regulates genome ploidy through ubiquitin–proteasome-mediated degradation of the CDK inhibitor rum1 and the S-phase initiator cdc18. *Genes Dev.*, **11**, 1548–1560.

Labib,K. and Moreno,S. (1996) rum1: a CDK inhibitor regulating G_1 progression in fission yeast. *Trends Cell Biol.*, **5**, 62–66.

Labib,K., Moreno,S. and Nurse,P. (1995) Interaction of cdc2 and rum1 regulates Start and S-phase in fission yeast. *J. Cell Sci.*, **108**, 3285–3294.

Lanker,S., Valdivieso,M.H. and Wittenberg,C. (1996) Rapid degradation of the G_1 cyclin Cln2 induced by CDK-dependent phosphorylation. *Science*, **271**, 1597–1601.

Martín-Castellanos,C., Labib,K. and Moreno,S. (1996) B-type cyclins regulate G_1 progression in fission yeast in opposition to the $p25^{rum1}$ CDK inhibitor. *EMBO J.*, **15**, 839–849.

Mathias,N., Johnson,S.L., Winey,M., Adams,A.E.M., Goetsch,L., Pringle,J.R., Byers,B. and Goebl,M.G. (1996) Cdc53 acts in concert with Cdc4p and Cdc34p to control the G_1-to-S phase transition and identifies a conserved family of proteins. *Mol. Cell. Biol.*, **16**, 6634–6643.

Maundrell,K. (1989) *nmt1* of fission yeast: a highly transcribed gene completely repressed by thiamine. *J. Biol. Chem.*, **265**, 10857–10864.

Mirabito,P.M. and Morris,N.R. (1993) BIMA, a TPR-containing protein required for mitosis, localizes to the spindle pole body in *Aspergillus nidulans*. *J. Cell Biol.*, **120**, 959–968.

Monderset,O., McGowan,C.H. and Russell,P. (1996) Cig2, a B-type cyclin, promotes the onset of S in *Schizosaccharomyces pombe*. *Mol. Cell. Biol.*, **16**, 1527–1533.

Moreno,S. and Nurse,P. (1990) Substrates for $p34^{cdc2}$: *in vivo veritas*? *Cell*, **61**, 549-–551.

Moreno,S. and Nurse,P. (1994) Regulation of progression through the G_1 phase of the cell cycle by the *rum1*$^+$ gene. *Nature*, **367**, 236–242.

Moreno,S., Hayles,J. and Nurse,P. (1989) Regulation of $p34^{cdc2}$ protein kinase during mitosis. *Cell*, **58**, 361–372.

Moreno,S., Klar,A. and Nurse,P. (1991) Molecular genetic analysis of fission yeast *Schizosaccharomyces pombe*. *Methods Enzymol.*, **194**, 793–823.

Moreno,S., Labib,K., Correa,J. and Nurse,P. (1994) Regulation of the cell cycle timing of start in fission yeast by the *rum1*$^+$ gene. *J. Cell Sci. Suppl.*, **18**, 63–68.

Murray,A.W. (1995) Cyclin ubiquitination: the destructive end of mitosis. *Cell*, **81**, 149–152.

Murray,A.W. and Kirschner,M.W. (1989) Cyclin synthesis drives the early embryonic cell cycle. *Nature*, **339**, 275–280.

Murray,A.W., Solomon,M.J. and Kirschner,M.W. (1989) The role of cyclin synthesis and degradation in the control of maturation promoting factor activity. *Nature*, **339**, 280–286.

Musti,A.M., Treier,M., Peverali,F.A. and Bohman,D. (1986) Differential regulation of c-Jun and JunD by ubiquitin-dependent protein degradation. *Biol. Chem.*, **377**, 619–624.

Nasmyth,K. (1993) Control of the yeast cell cycle by the Cdc28 protein kinase. *Curr. Opin.Cell Biol.*, **5**, 166–179.

Nasmyth,K. (1996) At the heart of the budding yeast cell cycle. *Trends Genet.*, **12**, 405–412.

Nugroho,T.T. and Mendenhall,M.D. (1994) An inhibitor of yeast cyclin-dependent protein kinase plays an important role in ensuring the genomic integrity of daughter cells. *Mol. Cell. Biol.*, **14**, 3320–3328.

Nurse,P. (1975) Genetic control of cell size at cell division in yeast. *Nature*, **256**, 547–551.

Nurse,P. (1994) Ordering S-phase and M-phase in the cell cycle. *Cell*, **79**, 547–550.

Nurse,P. and Bissett,Y. (1981) Gene required in G_1 for commitment to cell cycle and in G_2 for control of mitosis in fission yeast. *Nature*, **292**, 558–560.

Obara-Ishihara,T. and Okayama,H. (1994) A B-type cyclin negatively regulates conjugation via interacting with cell cycle 'start' genes in fission yeast. *EMBO J.*, **13**, 1863–1872.

O′Donnell,K.L., Osmani,A.H., Osmani,S.A. and Morris,N.R. (1991) bimA encodes a member of the tretratricopeptide repeat family of proteins and is required for the completion of mitosis in *Aspergillus nidulans*. *J. Cell Sci.*, **99**, 711–719.

Pagano,M., Tam,S.W., Theodoras,A.M., Beer-Romero,P., Del Sal,G., Chau,V., Yew,P.R., Draetta,G.F. and Rolfe,M. (1995) Role of the ubiquitin–proteasome pathway in regulating abundance of the cyclin-dependent kinase inhibitor p27. *Science*, **269**, 682–685.

Pahl,H.L. and Baeuerle,P.A. (1996) Control of gene expression by proteolysis. *Curr. Opin. Cell Biol.*, **8**, 340–347.

Pardee,A. (1974) A restriction point for control of normal animal cell proliferation. *Proc. Natl Acad. Sci. USA*, **71**, 1286–1290.

Peter,M. and Herskowitz,I. (1994) Direct inhibition of the yeast cyclin-dependent kinase cdc28–cln by Far1. *Science*, **265**, 1228–1231.

Peter,M., Gartner,A., Horecka,J., Ammerer,G. and Herskowitz,I. (1993) FAR1 links the signal transduction pathway to the cell cycle machinery in yeast. *Cell*, **73**, 747–760.

Picard,A., Galas,S., Peaucellier,G. and Dorée,M. (1996) Newly assembled cyclinB–cdc2 kinase is required to suppress DNA replication between meiosis I and meiosis II is starfish oocytes. *EMBO J.*, **15**, 3590–3598.

Piggott,J.R., Rai,R. and Carter,B.L.A. (1982) A bifunctional product involved in two phases of the yeast cell cycle. *Nature*, **298**, 391–393.

Reed,S.I and Wittenberg,C. (1990) Mitotic role for the Cdc28 protein kinase of *Saccharomyces cerevisiae*. *Proc. Natl Acad. Sci. USA*, **87**, 5697–5701.

Rogers,S., Wells,R. and Rechsteiner,M. (1986) Amino acid sequences common to rapidly degraded proteins: the PEST hypothesis. *Science*, **234**, 364–368.

Samejima,I. and Yanagida, M. (1994) Bypassing anaphase by fission yeast *cut9* mutation—requirement of *cut9*$^+$ to initiate anaphase. *J. Cell. Biol.*, **127**, 1655–1670.

Sauer,K., Knoblich,J.A., Richardson,H. and Lehner,C.F. (1995) Distinct modes of cyclinE/cdc2c kinase regulation and S-phase control in mitotic and endoreduplication cycles of *Drosophila* embryogenesis. *Genes Dev.*, **9**, 1327–1339.

Sazer,S. and Sherwood,S.W. (1990) Mitochondrial growth and DNA synthesis occur in the absence of nuclear DNA replication in fission yeast. *J. Cell Sci.*, **97**, 509–516.

Sherr,C.J. and Roberts,J.M. (1995) Inhibitors of mammalian G_1 cyclin-dependent kinases. *Genes Dev.*, **9**, 1149–1163.

Schneider,B.L., Yang,Q.-H. and Futcher,A.B. (1996) Linkage of replication to Start by the Cdk inhibitor Sic1. *Science*, **272**, 560–562.

Schwob,E., Böhm,T., Mendenhall,M. and Nasmyth,K. (1994) The B-type cyclin kinase inhibitor $p40^{SIC1}$ controls the G_1 to S transition in *S.cereviasiae*. *Cell*, **79**, 233–244.

Stern,B. and Nurse,P. (1996) A quantitative model for the cdc2 control of S-phase and mitosis in fission yeast. *Trends Genet.*, **12**, 345–350.

Stuart,D. and Wittenberg,C. (1995) CLN3, not positive feedback, determines the timing of CLN2 transcription in cycling cells. *Genes Dev.*, **9**, 2780–2794.

Sudakin,V., Ganoth,D., Dahan,A., Heller,H., Hershko,J., Luca,F.C., Ruderman,J.V. and Hershko,A. (1995) The cyclosome, a large complex containing cyclin-selective ubiquitin ligase activity, targets cyclins for destruction at the end of mitosis. *Mol. Biol. Cell*, **6**, 185–197.

Thanos,D. and Maniatis,T. (1995) NF-κB: a lesson in family values. *Cell*, **80**, 529–532.

Traenkner,E.B.-H., Pahl,H.L., Henkel.,T., Schmidt,K.N., Wilk,S. and Baeuerle,P. (1995) Phosphorylation of human IκB-α on serine 32 and 36 controls IκB-α proteolysis and NF-κB activation in response to diverse stimuli. *EMBO J.*, **14**, 2876–2883.

Treier,M., Staszewski,L.M. and Bohman,D. (1994) Ubiquitin-dependent c-Jun degradation *in vivo* is mediated by the ¶ domain. *Cell*, **78**, 787–798.

Tugendreich,S., Tomkiel,J.W., Earnshaw,J. and Hieter,P. (1995) CDC27Hs colocalizes with CDC16Hs to the centrosome and mitotic spindle and is essential for the metaphase to anaphase transition. *Cell*, **81**, 261–268.

Tyers,M., Tokiwa,G., Nash,R. and Futcher,B. (1992) The Cln3–Cdc28 kinase complex of *S.cerevisiae* is regulated by proteolysis and phosphorylation. *EMBO J.*, **11**, 1773–1784.

Van der Geer,P. and Hunter,T. (1994) Phosphopeptide mapping and phosphoamino acid analysis by electrophoresis and chromatography on thin-layer cellulose plates. *Electrophoresis*, **15**, 544–554.

Verma,R., Feldman,R.M.R. and Deshaies,R.J. (1997) SIC1 is ubiquitinated *in vitro* by a pathway that requires CDC4, CDC34 and cyclin/CDK activities. *Mol. Biol. Cell*, **8**, 1427–1437.

Willems,A.R., Lanker,S., Patton,E.E., Craig,K.L., Nason,T.F., Mathias,N., Kobayashi,R., Wittenberg,C. and Tyers,M. (1996) Cdc53 targets phosphorylated G_1 cyclins for the degradation by the ubiquitin proteolytic pathway. *Cell*, **86**, 453–463.

Wittenberg,C., Sugimoto,K. and Reed,S.I. (1990) G_1-specific cyclins of *S.cerevisiae*: cell cycle periodicity, regulation by mating pheromone and association with the $p34^{CDC28}$ protein kinase. *Cell*, **62**, 225–237.

Won,K.-A. and Reed,S.I. (1996) Activation of cyclinE/CDK2 is coupled to site-specific autophosphorylation and ubiquitin-dependent degradation of cyclin E. *EMBO J.*, **15**, 37–44.

Wuarin,J. and Nurse,P. (1996) Regulating S phase: CDKs, licensing and proteolysis. *Cell*, **85**, 785–787.

Yaglom,J., Linskens, M.H., Sadis,S., Rubin,D.M., Futcher,B., and Finley,D. (1995) $p34^{Cdc28}$-mediated control of Cln3 cyclin degradation. *Mol. Cell. Biol.*, **15**, 731–741.

Yamano,H., Ishii,K. and Yanagida, M. (1994) Phosphorylation of dis2 protein phosphatase at the C-terminal cdc2 consensus and its potential role in cell cycle regulation. *EMBO J.*, **13**, 5310–5318.

Yamano,H., Gannon,J. and Hunt,T. (1996) The role of proteolysis in cell cycle progression in *Schizosaccharomyces pombe*. *EMBO J.*, **15**, 5268–5279.

Yochem,J. and Byers,B. (1987) Structural comparison of the yeast cell division cycle gene *CDC4* and a related pseudogene. *J. Mol. Biol.*, **195**, 233–245.

Received June 19, 1997; revised October 20, 1997; accepted October 29, 1997